Study on the Stability and Performance of Algal-bacterial Granular Symbiosis System by Using Sequencing Batch Reactor

January 2019

Ziwen ZHAO

Study on the Stability and Performance of Algal-bacterial Granular Symbiosis System by Using Sequencing Batch Reactor

A Dissertation Submitted to
the Graduate School of Life and Environmental Sciences,
the University of Tsukuba
in Partial Fulfillment of the Requirements
for the Degree of Doctor of Philosophy in Environmental Studies
(Doctoral Program in Sustainable Environmental Studies)

Ziwen ZHAO

Abstract

Low chemical oxygen demand to nitrogen (COD/N) ratio in real domestic wastewater is becoming one of the most important and limiting factors for efficient nutrients removal during biological wastewater treatment. Besides, high energy consumption by aeration in conventional wastewater treatment plants (WWTPs) is also a great burden to the sustainable management of wastewater treatment. Algal-bacterial symbiosis system for wastewater treatment has been paid much attention due to its advantages like lower energy demand for organics degradation, enhanced nutrients removal, and more potential for resources recovery. However, algae harvesting and separation from the treated water is always a big challenge due to its small size, poor settleability and low density. On the other hand, aerobic granular sludge (AGS) with enhanced settleability and greater biomass retention is a promising biotechnology for wastewater treatment, while granular stability during long-term operation is still challenging its practical applications. In this context, algal-bacterial granular system, the combination of algae with AGS biotechnology, is proposed as a better solution for nutrients removal with less energy consumption. Previous research works clearly show that algal-bacterial granular consortia possesses compact granular structure and good biomass settleability. This study focused on the changes in granular stability and nutrients removal during wastewater treatment under low COD/N ratio or no air bubbling condition, especially on phosphorus (P) accumulation/ bioavailability of algal-bacterial AGS. In addition, the formation of algal-bacterial AGS from mature bacterial AGS were also attempted.

In this study, mature bacterial or algal-bacterial granules instead of activated sludge were used as seed sludge due to the expected shorter start-up time by using sequencing batch reactors (SBRs). The algal-bacterial AGS was cultivated from mature bacterial AGS, and compared with the bacterial AGS system regarding granular stability, nutrients removal and P accumulation/bioavailability. Major results can be summarized as follows:

(1) The algal-bacterial AGS system could be successfully developed by seeding mature bacterial AGS under light illumination with no algae inoculation. The mature algal-bacterial granules exhibited a compact structure with high stability, large size, and good settling properties. Moreover, relatively higher total nitrogen (TN, averagely 54.6%) and total phosphorus (TP, averagely 58.4%) removal efficiencies were achieved in the algal-bacterial AGS system, in comparison to 48.3% and 54.5% respectively in the bacterial AGS system. More importantly, compared with the P content (36.8 mg/g-SS) and P bioavailability (85%) of

bacterial granules, higher P content (44.2 mg/g-SS) with higher P bioavailability (92%) was detected in the algal-bacterial granules, indicating its high potential for P recovery to serve multipurposes.

(2) When the influent COD/N stepwise decreased from 8 to 1, the algal-bacterial AGS could maintain its granular stability and nutrients removal performance. Results showed that the integrity coefficient of the granules in the tested algal-bacterial AGS reactor stabilized at 0.7-5.4% when coping with the varying strength of influent wastewater, even at low COD/N ratio like COD/N = 1. It was also found that the lower influent COD/N ratio (2 and 1) might negatively impact the nitritation process in the algal-bacterial AGS system. The algal-bacterial AGS biomass was detected to have high P content (28.3 mg/g-SS) as well as extremely high P bioavailability (up to 98%) under the low influent carbon condition (COD/N = 1).

(3) The stability of algal-bacterial AGS was also examined in shaking photoreactors instead of air bubbling usually applied for AGS systems. The preliminary results indicate that the algal-bacterial AGS with good granular integrity (~ 8.4%) can produce low dissolved organic carbon (DOC, < 14 mg/L) effluent with high TN removal (66.9-76.1%). The large fluctuation in TP removal (15.1-71.6%) might be attributable to the designed light/dark cycle and hydraulic/sludge retention time, while the high P bioavailability (92%) was still maintained in the algal-bacterial AGS. Mechanisms involved in this system are demanding for better design of this kind of no air bubbling system, targeting more nutrients removal with less or no additional energy consumption.

Results from this study are expected to provide important and scientific data for the design and realization of algal-bacterial AGS application in practice.

Key words: Algal-bacterial aerobic granular sludge; Low carbon wastewater; Granular stability; Nutrients removal; Phosphorus accumulation/bioavailability

Contents

List of tables

List of figures

Abbreviations

AGS	Aerobic granular sludge
AOB	Ammonia oxidizing bacteria
AP	Apatite phosphorus
AS	Activated sludge
COD	Chemical oxygen demand
DIC	Dissolved inorganic carbon
DO	Dissolved oxygen
DOC	Dissolved organic carbon
DTC	Dissolved total carbon
EPS	Extracellular polymeric substances
GHGs	Greenhouse gases
HRT	Hydraulic retention time
IP	Inorganic phosphorus
LB-EPS	Loosely bound extracellular polymeric substances
LB-PN	Loosely bound proteins
LB-PS	Loosely bound polysaccharides
MLSS	Mixed liquor suspended solids
MLVSS	Mixed liquor volatile suspended solids
N	Nitrogen
NAIP	Non-apatite inorganic phosphorus
NaAc	Sodium acetate
NOB	Nitrite oxidizing bacteria
O_2	Oxygen
OP	Organic phosphorus
P	Phosphorus
PAOs	Polyphosphate-accumulating organisms
PCR	Polymerase chain reaction
PN	Proteins
PS	Polysaccharides
SAUR	Specific ammonia uptake rate
SBRs	Sequencing batch reactors

SMT	Standards, Measurements and Testing
SNUR	Specific nitrite uptake rate
SOUR	Specific oxygen utilization rat
SRT	Sludge retention time
SS	Suspended solids
SVI	Sludge volume index
TAN	Total ammonia nitrogen
TB-EPS	Tightly bound extracellular polymeric substances
TB-PN	Tightly bound proteins
TB-PS	Tightly bound polysaccharides
TN	Total nitrogen
TP	Total phosphorus
VSS	Volatile suspended solids
WAS	Waste activated sludge
WWTPs	Wastewater treatment plants

Chapter 1 Introduction

1.1 Aerobic granular sludge

Activated sludge (AS) process is the most commonly applied biological wastewater treatment technology, and it is still at the heart of current sewage treatment technology though this process has been presented since 1912 (van Loosdrecht and Brdjanovic, 2014). However, AS process has several drawbacks. For instance, aeration processes are energy-intensive, requiring 60-65% from total energy consumption, which approximately occupying at least one third of the total operating cost of a conventional wastewater treatment plant (WWTP) (Fernandez et al., 2011). Settling tanks and recycling systems are essential due to the poor settling ability of AS. Moreover, there are still problems relating to the treatment of waste activated sludge (WAS) and its large land area occupation. To overcome these disadvantages, more feasible and innovative technologies for wastewater treatment have been developed during the last decades.

Aerobic granular sludge (AGS) is regarded as one promising biotechnology, which possesses many incomparable advantages compared to conventional AS, such as dense and compact structure, excellent settleability, and high tolerance to toxicity and loading rate (Adav et al., 2008; Pronk et al., 2015). Aerobic granules were first reported by Mishima and Nakamura (1991) in a continuous upflow aerobic sludge blanket bioreactor. In the late 1990s, Morgenroth et al. (1997) used a sequencing batch reactor (SBR) to develop AGS and the granular sludge was formed after 40 days' cultivation. Since then, extensive research work has been conducted by using AGS to treat wastewaters containing various organics, nitrogen (N), phosphorus (P), and toxic substances. To date, AGS with efficient removal of pollutants and lower operation costs has been successfully applied in large-scale domestic and industrial WWTPs (Li et al., 2014; Pronk et al., 2015; Świątczak and Cydzik-Kwiatkowska, 2018).

Despite the significant advancements in the development of AGS process, long start-up periods of granulation and loss of granular stability during long-term operation are reported as the main crucial barriers to its practical applications (Zhang et al., 2016a). During the past two decades, much effort has been put into acceleration of the start-up of aerobic granules such as adding metal ions or external carrier media and manipulating operational conditions. So far, the start-up period of aerobic granulation could be greatly shortened. For instance, Liu and Tay (2015) reported that clear granules could be formed within 24 hours through applying strong hydraulic selection pressure with overstressed organic loading rate (OLR). However, the loss

of granular stability during long-term operation remains unsolved. Lee et al. (2010) pointed out the problems regarding the instability of granules and summarized some mechanisms involved, including outgrowth of filamentous organisms, hydrolysis of the anaerobic core, function loss of some strains, decrease in extracellular polymeric substances (EPS), and so on. Up to now, the mechanisms behind the loss of AGS stability have not been fully understood. Therefore, one of the current challenges for the large-scale application of AGS technology is to find the suitable operating conditions to maintain the long-term granular stability.

1.2 Algal-bacterial aerobic granular sludge

Excessive amounts of nutrients in water bodies can lead to environmental issues like eutrophication, especially algal blooms. Algae growth can also be observed in wastewater treatment units and receives the interest of researches due to their capacity for nutrients uptake as well as simultaneous oxygen (O_2) production (Li et al., 2015). It is well known that algal-bacterial consortia system is regarded as a competitive alternative to conventional AS process due to its unique features such as less energy demand for degradation of organic matter, enhanced nutrients removal, and higher potential for resources recovery (Quijano et al., 2017; Sforza et al., 2018). However, algae harvesting and separation from the treated water is challenging the promising algal-bacterial consortia systems due to the small size of microalgae cells (3-30 μm), poor settleability and low density (Zhou et al., 2017; Hu et al., 2017). Recently, there's a growing interest in the use of innovative solutions to combine microalgae technology with AGS process, aiming to solve this problem. Previous works show that algae could naturally grow during granulation process under sunlight exposure and stably co-exist with AGS in SBRs (Huang et al., 2015a; Li et al., 2015), and the resultant symbiosis system reflects a prospective option for more nutrients uptake or removal compared with the AS process-based wastewater treatment. In addition, the algal-bacterial granular symbiosis system can be successfully achieved by using mature AGS (Liu et al., 2017) or 50% (w/w) algal-bacterial granules in continuous-flow reactors (Ahmad et al., 2017). Most recently, many reports claimed that enhanced system stability and improved nutrients removal efficiency could be achieved by using the algal-bacterial consortium in lab-scale photobioreactors (Zhang et al., 2018; Liu et al., 2018a, He et al., 2018; Meng et al., 2019).

Previous research works clearly show that algal-bacterial AGS is becoming a promising biotechnology for wastewater treatment due to its good sludge settleability, efficient nutrients removal and enhanced granular stability. However, previous works mainly focused on how to

form this kind of algal-bacterial AGS system. More and further studies regarding the impact of various operation conditions are still needed to provide scientific data for the design and realization of algal-bacterial AGS application in practice.

1.3 Phosphorus resource and fractionation

Phosphorus (P), a non-substitutable component in all living plants and organisms, is a crucial element to life. However, global reserves of high-quality phosphate rock are limited, and the current global reserves may be depleted in 50-100 years (Cordell et al., 2009). Therefore, recovering P from P-rich resources is particularly important. In recent years, many researches concentrated on P recovery from sewage sludge produced from wastewater treatment due to its high P content (Ye et al., 2016). In addition, previous reports demonstrated that algal biomass produced from wastewater treatment can serve as P fertilizer in agriculture (Mulbry et al., 2005; Mulbry et al., 2007). Moreover, high content of P could be accumulated in the AGS resulting in P-rich aerobic granules obtained from simultaneous nitrification and denitrification processes (Lin et al., 2012). Thus, algal-bacterial AGS potentially can be used for P recovery, which can reduce the global phosphate rock demand to a great extent.

P in granules, namely total phosphorus (TP), organic phosphorus (OP), inorganic phosphorus (IP), non-apatite inorganic phosphorus (NAIP) and apatite phosphorus (AP), can be fractioned and quantified using the Standards, Measurements and Testing (SMT) Programme extraction protocol (Ruban et al., 1999). According to Huang et al. (2015b), NAIP is mainly composed of the fraction associated with Al, Fe and Mn, which together with OP is regarded as bioavailable P that can be potentially released and utilized by microorganisms and plants. AP is the Ca-bound P that is hard to be utilized by microorganisms and plants. Solovchenko et al. (2016) claimed that P is often presented in a form that does not meet specifications for agricultural use when being recovered chemically or biologically from wastewater. Thus, more detailed information on P fraction in granular sludge is necessary. As reported, the proportion of (NAIP + OP) to TP for AS, bacterial AGS and algae granule was about 80%, 80% and 92% respectively (Huang et al., 2015b; Cai et al., 2019). This suggests the high P bioavailability might be achieved in the algal-bacterial AGS, which is beneficial for P recovery. Up to the present, still, very limited information is available regarding P content and its bioavailability in algal-bacterial AGS.

1.4 Carbon source in wastewater treatment

It is well known that carbon source present in wastewaters is a key factor affecting the performance of nutrients removal (N and P) during biological wastewater treatment. However, real municipal wastewater and/or its combination with industrial wastewaters is always characterized with an extremely low carbon concentration, especially in South China (Wang et al., 2017). Thus, it is a big challenge to maintain highly efficient nutrients removal in WWTPs due to the lack of carbon source in wastewaters (Gong et al., 2018). Many innovations have been attempted to enhance the nutrients removal in municipal WWTPs with reduced consumption of carbon source, like two-sludge system (Wang et al., 2017) or coupling electrolysis with an anaerobic-anoxic-oxic (A^2/O) reactor (Gong et al., 2018). As it is known, COD/N ratio of wastewater is an important operation parameter for the stable operation of biotechnology-based WWTPs, which might affect granular stability. A previous study explored the impact of COD/N ratio on AGS disintegration (Luo et al., 2014). Their results showed that decrease in COD/N ratio from 4 to 1 brought about the reduction of net tyrosine production in extracellular polymeric substances (EPS) and the shift of major microbial communities, leading to the decreases in nitrification efficiency and physical strength, size and settleability of AGS, thus the collapse of AGS structure. Moreover, Kocaturk and Erguder (2016) claimed that in terms of high COD and total ammonia nitrogen (TAN) removals and granular stability, the optimum COD/N ratio was about 7.5. These results indicate that insufficient carbon source might limit the application of AGS into practice.

The N and P uptake by algae enables the algal-bacterial symbiosis system to realize desirable nutrients removal from wastewater without external carbon sources (Lee et al., 2015; Tang et al., 2016). Thus, the requirement of carbon source for nutrients removal might be reduced owing to the co-existence of algae in the algal-bacterial granular system. Up to the present, however, the impact of carbon source on the algal-bacterial AGS system has not been paid much attention, even though this system is most promising for enhanced nutrients removal with less carbon source requirement.

1.5 Energy consumption in aeration process

Aeration process is an essential step for most WWTPs and accounts for the largest part of total energy costs in WWTP, ranging from 45 to 75% of the energy consumption depending on the processes applied (Rosso et al., 2008). For example, in a AS process-based WWTP, up to 60% of the energy consumption is contributed by aeration units which provide O_2 necessary for

the growth of aerobic bacteria (Boelee et al., 2014). Compared with the AS process-based WWTP, an AGS process-based WWTP in the Netherlands consumed 58-63% less total energy mainly due to the lack of mixers, conventional recycle pumps, settlers and sludge return pumps. It was estimated that 5-10% of energy saving was achieved in aeration part (Pronk et al., 2015).

In the algal-bacterial symbiosis system, the growing algae generate O_2 which is required by aerobic bacteria for degradation of organic matter; at the same time nutrients and carbon dioxide (CO_2) produced from oxidation can be assimilated by algae (Santiago et al., 2013). Therefore, the application of algal-bacterial AGS for potentially less energy consumption during wastewater treatment, especially in aeration units, has become a research hotspot. Tiron et al. (2015) claimed that the activated algae granular system could efficiently remove organic matter and nutrients from low-strength wastewater with O_2 being provided only by algae through photosynthesis. Most recently, Abouhend et al. (2018) attempted oxygenic photogranules in stirred-tank reactors with no aeration to treat wastewater, achieving efficient removals of COD and N. Although many efforts have been devoted to the algal-bacterial granular system, especially on energy saving via less aeration or no aeration, previous works mainly focused on organics or nutrients removal efficiencies under the tested conditions. To the best of our knowledge, the stability of algal-bacterial granules in shaking photoreactors instead of air bubbling systems usually applied for AGS and algal-bacterial AGS process, which are closely related with practical application of this technology, has not been documented yet.

1.6 Research objectives and originality

As described above, low COD/N ratio in real domestic wastewater is becoming one of the most important and limiting factors for efficient nutrients removal during biological wastewater treatment. Besides, high energy consumption by aeration in conventional WWTPs is also a great burden to the sustainable management of wastewater treatment. And most recently, algal-bacterial AGS, the combination of algae with AGS biotechnology, is proposed as a better solution for nutrients removal with less carbon source requirement and energy consumption. Nevertheless, the impact of low COD/N wastewater or no air bubbling condition on the new algal-bacterial AGS system has not been paid much attention. Therefore, the objectives of this study were to investigate the changes in granular stability and nutrients removal during wastewater treatment under low COD/N wastewater or no air bubbling condition, especially on P accumulation/bioavailability of algal-bacterial AGS. In addition, the formation of algal-bacterial AGS from mature bacterial AGS were also attempted. Results from this study are

expected provide important and scientific data for the design and realization of algal-bacterial AGS application in practice.

1.7 Structure of the thesis

The structure of the thesis is illustrated by the research framework shown in Figure 1-1. The main contents of each chapter in this thesis can be summarized as follows.

An overview was given in Chapter 1 on bacterial AGS and algal-bacterial AGS systems, including recent achievements and problems. The environment issues related with P resource and fractionation, carbon source in wastewater, and energy consumption in aeration process were also presented. Finally, the objectives of this study and structure of the thesis were arrived in this chapter.

The formation of algal-bacterial AGS from mature bacterial AGS was conducted in Chapter 2, together with evaluation on its granular stability and nutrients removal performance. Additionally, P accumulation and its bioavailability in bacterial AGS and algal-bacterial AGS were also compared. Finally, the changes in microbial biodiversity of bacterial AGS and algal-bacterial AGS were analyzed to shed light on the mechanisms involved.

The effect of decrease in wastewater COD/N ratio (from 8 to 1) was investigated with respect to granular stability, nutrients removal and accumulation of the algal-bacterial AGS. The granular morphology, strength and extracellular polymeric substances (EPS) content were determined and analyzed. In addition, P accumulation and its bioavailability in algal-bacterial granules were also explored in this chapter.

A preliminary trial was attempted in Chapter 4 on the characteristics and performance of the mature algal-bacterial AGS in shaking photoreactors instead of air bubbling systems. Besides, P accumulation and its bioavailability in the algal-bacterial granules were detected in no air bubbling systems.

At last, the main findings of this research were summarized in Chapter 5. For better application of algal-bacterial AGS process, future studies were also proposed.

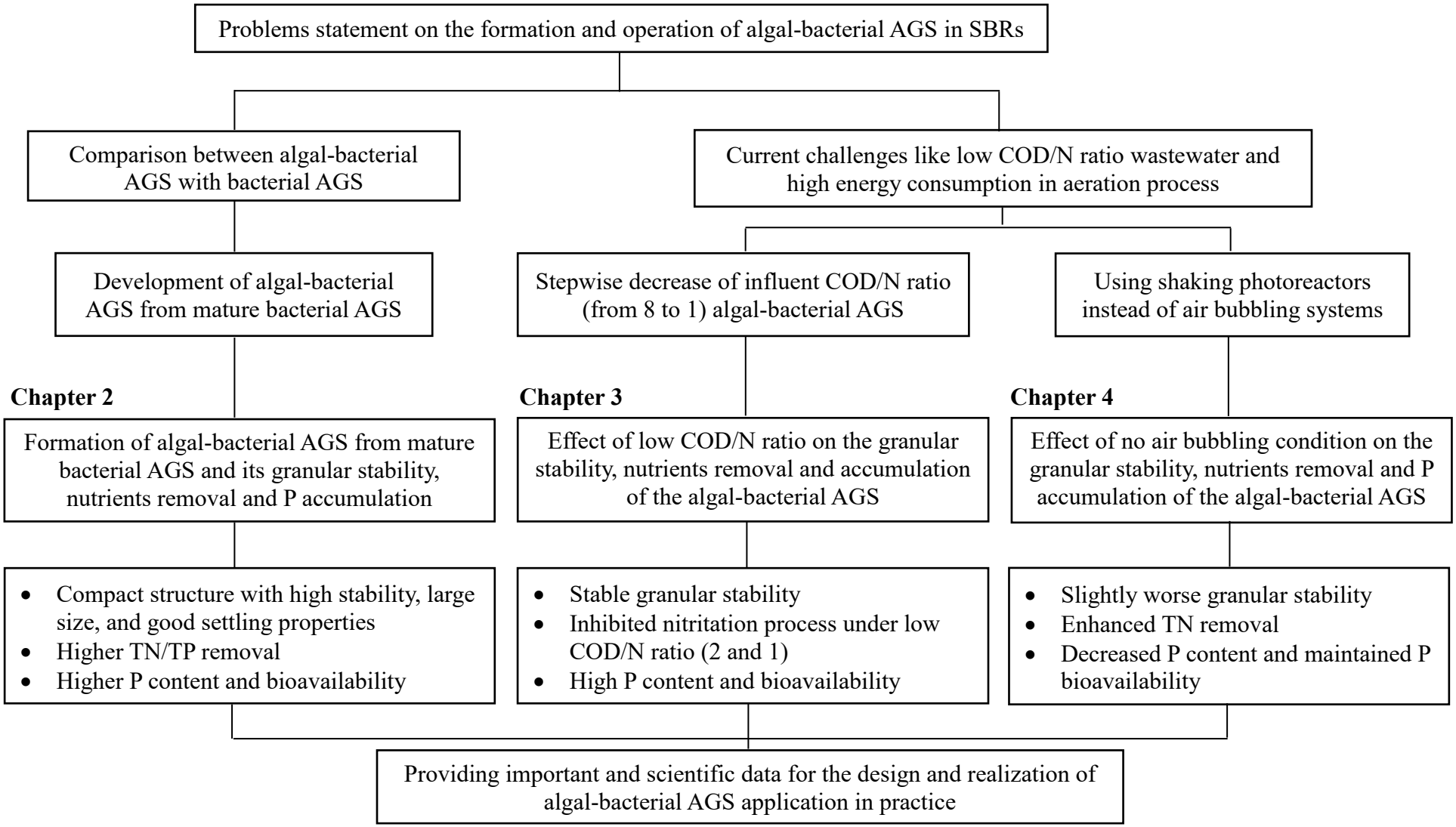

Figure 1-1 Research framework of this study.

Chapter 2 Formation of algal-bacterial AGS from mature bacterial AGS and its granular stability, nutrients removal and P accumulation

2.1 Introduction

Wastewater treatment by means of algal-bacterial granules has become a hot topic worldwide recently. Previous studies have characterized the algal-bacterial granules and bacterial communities (He et al., 2018; Zhang et al., 2018). Up to present, however, very few works documented on the comparison between the conventional bacterial AGS and algal-bacterial AGS, especially P content and its bioavailability.

Therefore, the objective of this study was to investigate the stability, nutrients removal performance and P fraction of algal-bacterial AGS. The morphology, characteristics and nutrients removal of the algal-bacterial granules were observed and analyzed. Additionally, P fraction and its bioavailability in the granules were also analyzed and compared between the bacterial AGS and algal-bacterial AGS systems. Finally, changes in microbial biodiversity in the granules were analyzed to shed light on the mechanisms involved in the algal-bacterial AGS system. It is expected that this work would provide scientific and meaningful references for performance and stability enhancement as well as P recovery of algal-bacterial AGS system in practice.

2.2 Materials and methods

2.2.1 Experimental set-up and operation conditions

The experiments were conducted in two identical cylindrical SBRs, i.e., Rc (Control, without artificial sunlight) and Rs (under artificial sunlight) (D = 54 mm and H = 500 mm with a working volume of 0.92 L each). In this study, Rs was operated under illumination of an artificial solar light fixed at 12 h/12 h (day/night). The light was located on the top of the reactor with light illuminance of approximately 7200 lux on the surface of water in the reactor. A black plastic bag was used to cover the light together with the reactors to prevent their additional exposure to the room light. The two reactors were operated at room temperature (25 ± 2°C) under alternatively anaerobic and aerobic conditions with a cycle duration of 4 h. Each cycle consisted of 2 min filling, 45 min non-aeration period, 188 min aeration period, 2 min settling, and 3 min effluent discharge. During aeration, air was provided by an air pump (AK-40, KOSHIN, Japan) from the bottom of reactors through air bubble diffusers at an air flow rate of 0.55 cm/s. All these operations were performed automatically by the timer-controlled pumps.

The volumetric exchange ratio was kept at 53%, resulting in a hydraulic retention time (HRT) of about 7.5 h. Sludge retention time (SRT) was kept at approximately 30 days through controlled sludge discharge.

Mature aerobic granules used as seed sludge in this study were collected from a laboratory-scale SBR which has been stably operated for 320 days. The initial biomass concentration was averagely 3.01 g/L in mixed liquor suspended solids (MLSS) with a sludge volume index (SVI_5) of 39.6 mL/g.

Synthetic domestic wastewater used in these experiments consisted of 300 mg COD/L (sodium acetate), 5 mg PO_4^{3-}-P/L (KH_2PO_4), 50 mg NH_4^+-N/L (NH_4Cl), 10 mg Ca^{2+}/L ($CaCl_2$), 5 mg Mg^{2+}/L ($MgSO_4 \cdot 7H_2O$), 5 mg Fe^{2+}/L ($FeSO_4 \cdot 7H_2O$) and 1 ml/L of trace element solution. The composition of the trace elements solution was prepared according to Huang et al. (2015b). $NaHCO_3$ was added into the influent in order to maintain the influent pH at designated values (7.5-8.0). All the chemicals were supplied by Wako Pure Chemical Industries Ltd., Japan.

2.2.2 Analytical methods

Water samples were collected once every 5 days, and the sampling was done at the end of operation cycle during daytime. After filtration through 0.22 μm membrane, the filtrates were used for analysis. The determinations of mixed liquor (volatile) suspended solids (ML(V)SS), SVI, total nitrogen (TN), ammonia nitrogen (NH_4^+-N), nitrite nitrogen (NO_2^--N), nitrate nitrogen (NO_3^--N), and phosphorus (PO_4^{3-}-P) were conducted according to the standard methods (APHA, 2012). Dissolved organic carbon (DOC) was measured by the TOC analyzer (TOC-V_{CSN}, SHIMADZU, Japan) equipped with an auto-sampler (ASI-V, SHIMADZU, Japan). pH was determined by a compact pH meter (Horiba, Japan). Dissolved oxygen (DO) concentration in the bulk liquor was measured with a DO meter (DO-31P, DKK-TOA, Japan). A pocket digital lux meter (ANA-F11, Tokyo Photoelectric Co., Ltd., Japan) was used to measure light intensity in the reactors. The extraction and determination of chlorophyll *a* from granules were conducted using acetone and a spectrophotometry method described by Tang et al. (2016).

Granular size was measured by a stereo microscope (STZ-40TBa, SHIMADZU, Japan) with a program Motic Images Plus 2.3S (version 2.3.0). Morphological characteristics of the granules were observed using stereomicroscope (Leica M205 C Microscope, Leica Microsystems, Switzerland). The settling velocity was determined by placing individual granules in a graduated cylinder filled with tap water and measuring the time it took to drop

from a fixed height. At least 100 granules were sampled randomly for a single test, and the average values were used in this study. The strength of granules was expressed in terms of integrity coefficient (%) by a shock method as described by Ghangrekar et al. (2005), which was defined as the ratio of solids in the supernatant after being shaken on a platform shaker at 200 rpm for 5 min to the total weight of the granular sludge used for this test.

Microbial activity was indicated by specific oxygen uptake rate (SOUR) in this study. The measurement of SOUR was conducted in duplicate using the granules from both SBRs at each operation stage. A 25 mL granule sample, taken from each SBR at the end of aeration phase, was washed with deionized water for 3 times, and then mixed with 125 mL synthetic wastewater after being loaded into a 250 mL glass flask. Prior to the test, air was pumped into the flask till the DO increased to a relatively stable level. The DO level in the mixture was continuously recorded by the DO meter right from the moment when the aeration was stopped and at the same time the flask was sealed (leaving the DO meter inside). The SOUR value (mg O_2/g-VSS·h) was calculated from the DO reduction slope (along with the time after stopping aeration) and the concentration of MLVSS (Tang et al., 2016). Specific ammonia uptake rate (SAUR) and specific nitrite uptake rate (SNUR) were measured according to Huang et al. (2015a).

2.2.3 High-throughput sequencing analysis

The total DNA of granular sludge samples harvested on day 40 from Rc and Rs were extracted by using Mo-Bio PowerMax® Soil DNA Isolation Kit (MoBio Laboratories, Inc., USA) according to the manufacturer's protocol. The quality and quantity of the extracted DNA was assessed by a Nanodrop® 2000 spectrophotometer. After DNA extraction, polymerase chain reaction (PCR) and high-throughput sequencing and bioinformatics analysis were performed as described by Cai et al. (2016). The 16S rRNA gene sequencing primers were 338F (5′-ACTCCTAC GGGAGGCAGCAG-3′) and 806R (5′-GGACTACHVGGGTWTCTAAT-3′) with different barcodes for the V3-V4 region of the 16S rRNA gene. The 18S rRNA gene algal sequencing primers were p23SrVF (5′-GGACAGAAAGACCCTATGAA-3′) and p23SrVR (5′-TCAGCCTGTTATCCCTAGAG-3′). PCR was performed in ABI GeneAmp® 9700 (Applied Biosystems, USA) under the following conditions: 95°C for 3 min, followed by 35 cycles at 95°C for 30 s, 55°C for 30 s, 72°C for 45 s and a final extension step at 72°C for 10 min. After purification using the QIAquick PCR Purification Kit (Qiagen, Germany) and quantification using QuantiFluor-ST (Promega, USA), the PCR products of all samples were taken for high-throughput sequencing on an Illumina platform (Illumina PE250, USA).

MOTHUR (version: 1.31.2) was used for analyzing the biodiversity of bacteria and eukaryote in the granules.

2.3 Results and discussion

2.3.1 Granulation and characterization of the algal-bacterial AGS

(1) Morphology of granules

In this study, mature granules instead of activated sludge were used as seed sludge due to its expected shorter start-up time. The morphological changes of granules in Rc and Rs were observed and recorded during the experiment (Figure 2-1). At first, the mature granules were yellowish-brown in color and reflected irregular shape, compact and dense structure. Interestingly, from day 5, algae appeared on the inner wall of Rs, accelerating the formation of algal-bacterial AGS. After day 26, almost all granules in Rs turned into light green. Thereafter, algal-bacterial AGS turned to dark green in most parts of the granules. At the end of operation, the average chlorophyll *a* concentration of the granules in Rc and Rs were 0.2 and 3.6 mg/g-VSS, respectively (Table 2-1). This observation implies that algal-bacterial AGS system has been established successfully. However, more filamentous bacteria and algae on the surface of granules were observed in Rs under light illumination, which indicates algae growth directly influenced the biological community structure in the granules, thus may further influence other characteristics of granules as shown in the following experiments.

(2) Physical and chemical characteristics of granules

Samples were collected every 10 days to quantify the ML(V)SS, particle size, SVI_5, settling velocity, strength and chlorophyll *a* concentration (Table 2-1). An increased MLSS and MLVSS tendency was observed in both Rc and Rs during the operation. However, the MLSS or MLVSS concentrations increased from the initial 3.02 and 2.21 g/L to 5.21 and 4.08 g/L on day 40 in Rs, respectively, which were higher than those in Rc (3.98 and 2.93 g/L on day 40). A faster increase in biomass detected in Rs was mainly attributed to the growth of algae since much more increase in chlorophyll *a* concentration was detected in the granules from Rs. However, He et al. (2018) found that the growth of algae significantly decreased the MLSS and MLVSS in the reactor. The difference might be due to the short operation time (7 days) applied in this previous work (He et al., 2018), and their system might be still in the stabilization period. During the 40 days' operation, the average diameter of granules in Rc varied from 1.11 to 1.24 mm, while gradually increased from the initial 1.11 to 1.53 mm in Rs on day 40. These results

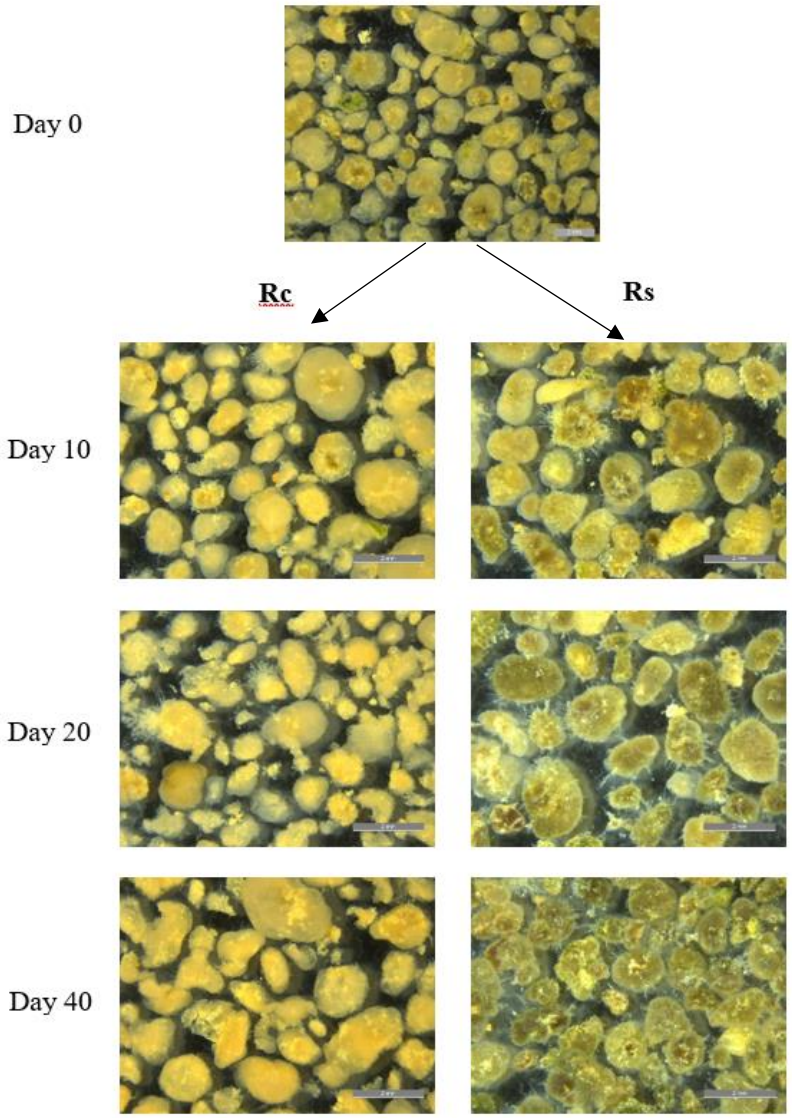

Figure 2-1 Morphological changes of the granules in the two reactors on day 0, 10, 20, and 40, respectively. Rc-the SBR without artificial sunlight, Rs-the SBR under artificial sunlight.

Table 2-1 Characteristics of granules from Rc and Rs during 40 days' operation (average values from duplicate tests).

Operating duration (day)	MLSS (g/L)		MLVSS (g/L)		Average diameter (mm)		SVI_5 (mL/g)		Settling velocity (m/h)		Integrity coefficient (%)		Chlorophyll *a* (mg/g-VSS)	
	Rc	Rs	Rc	Rs	Rc	Rs	Rc	Rs	Rc	Rs	Rc	Rs	Rc	Rs
0	2.97	3.02	2.18	2.21	1.11	1.11	39.6	39.4	28.7	28.7	10.7	10.7	0.3	0.3
10	3.31	3.52	2.41	2.55	1.24	1.52	45.6	43.9	30.9	30.4	15.0	7.9	0.3	1.1
20	3.62	4.27	2.62	3.25	1.23	1.47	46.8	43.2	32.8	34.0	12.1	0.9	0.2	1.9
30	3.82	4.85	2.84	3.72	1.14	1.54	46.6	44.0	31.7	33.7	12.2	2.6	0.2	2.9
40	3.98	5.21	2.93	4.08	1.19	1.53	46.0	44.5	33.4	36.5	11.1	2.7	0.2	3.6

Note: ML(V)SS-mixed liquor (volatile) suspended solids, SVI_5-sludge volume index at 5 min, Rc-the SBR without artificial sunlight, Rs-the SBR under artificial sunlight.

indicated that the growing algae in Rs exerted an obviously positive effect on the biomass growth rate and granular size.

As shown in Table 2-1, it was apparent that SVI_5 was stable at around 46 and 44 mL/g for the granules in Rc and Rs, respectively after 10 days' operation, suggesting the good settleability of algal-bacterial AGS could be maintained under light illumination. Moreover, as one of the most important advantages of the AGS technology, the settling velocity was found to averagely increase from the initial 28.1 m/h to 33.4 and 36.5 m/h at the end of the operation respectively for the granular sludge in Rc and Rs. The results showed that algal-bacterial AGS exhibited faster settling velocity or better settleability than conventional bacterial AGS (Rc), indicating algae growth plays a positive role in the enhancement of settling property of the granules.

The integrity coefficients of the granules in the two reactors during the 40 days' operation were also monitored (Table 2-1). Clearly seen, the integrity coefficient of algal-bacterial AGS in Rs ranged between 0.9% and 10.7% during the whole operation, which is much lower than those in Rc (10.7-15%), implying algal-bacterial AGS has better stability. This observation is different from Huang et al. (2015a) who noticed that the stability of aerobic granules was negatively affected by the growth of algae during the aerobic granulation when AS was used as seed sludge. This difference is most probably attributable to the different characteristics of seed sludge and influent as well as more illumination time applied in this study.

2.3.2 Overall performance on DOC and nutrients removal

(1) DOC and P removals

The changes in effluent DOC and TP concentration and removal efficiency in Rc and Rs are shown in Figure 2-2a and Figure 2-2b. The average removal efficiencies of DOC and TP were respectively 94.5 ± 1.6% and 58.4 ± 4.3% in Rs, and 93.8 ± 1.8% and 54.5 ± 3.6% in Rc during the 40 days' operation. This observation signaled that the algal-bacterial granular system has a potential advantage on the organics and TP removals compared to the conventional bacterial AGS. In addition, the higher granular SOUR of Rc (25.2 ± 0.2 mg-O_2/g-VSS·h) compared to that of Rs (18.9 ± 0.4 mg-O_2/g-VSS·h) at the end of operation has some implications: (1) Algae growth might negatively influence the organic matter degradation capacity of bacteria; (2) Algae growth may produce O_2 that decreases O_2 uptake from the surrounding environment by bacteria; (3) Most algae have lower bioactivity than bacteria as described by Huang et al. (2015a). However, He et al. (2018) and Zhang et al. (2018) found

that algae growth increased the SOUR of granules. The difference might be due to the different algae species grew or applied under different cultivation conditions among these research works.

The removal of P via chemical precipitation was unlikely occurred when the pH was lower than 9.0 in the reactor throughout the operation in all the reactors (Zhang et al., 2018). Therefore, it was assumed that biomass uptake was the main mechanism of phosphorus removal in this study. The TP removal efficiency in Rs was approximately 3.9% higher than that in Rc, which was attributable to the activity of polyphosphate-accumulating organisms (PAOs) and assimilation by algae in Rs. The cycle experiments were conducted in the two SBRs on day 32. As shown in Figure 2-3, the average anaerobic P release and aerobic P uptake in Rs were 2.2 and 0.57 mg/g-VSS·h, much lower than those in Rc (4.7 and 1.09 mg/g-VSS·h), suggesting the growth or activity of PAOs in Rs might be inhibited due to the growth of algae.

(2) Nitrogen removal

Figure 2-2c shows the changes of N species and N removal performance in Rc and Rs during the 40 days' operation. The granules in both Rc and Rs systems exhibited excellent performance in NH_4^+-N removal, achieving > 99% from the beginning of the operation. Moreover, only little amount of NO_2^--N in both reactors was detected, and NO_3^--N was found to be the dominant N species in the effluents from Rc and Rs. The lower NO_3^--N concentration in Rs (averagely 22.7 mg/L) relative to Rc (25.8 mg/L) indicated that denitrification was enhanced in the algal-bacterial AGS system. This observation is probably due to the increase in granular size as well as the enlarged anaerobic zone of algal-bacterial granules in this study. Similar phenomenon could be found in previous studies (Ahmad et al., 2017; Zhang et al., 2018).

In this study, TN concentration was calculated as the sum of NH_4^+-N, NO_2^--N and NO_3^--N in the reactor. Results show that TN removal efficiency was averagely 48.3 ± 2.1% and 54.6 ± 0.9% for Rc and Rs, respectively from day 20 to the end of the experiment. On the other hand, the SAUR and SNUR of the granules, representing the activity of nitrifying bacteria in the algal-bacterial granules, were measured by using the granules from the two reactors on day 40. The granular SAUR and SNUR values were much higher in Rs averagely 5.41 ± 1.2 and 5.39 ± 1.3 mg-N/g-VSS·h, than those (2.22 ± 0.2 and 2.51 ± 0.2 mg-N/g-VSS·h) in Rc, which suggested that algae growth enhanced the activity of nitrifying bacteria. Similar results were reported previously (Tang et al., 2016; Zhang et al., 2018), in which the addition of microalgae enhanced the activities of ammonia oxidizing bacteria (AOB) and nitrite oxidizing bacteria (NOB) under light illumination of 6000 lux or 121 μmol/m^2·s using SBRs.

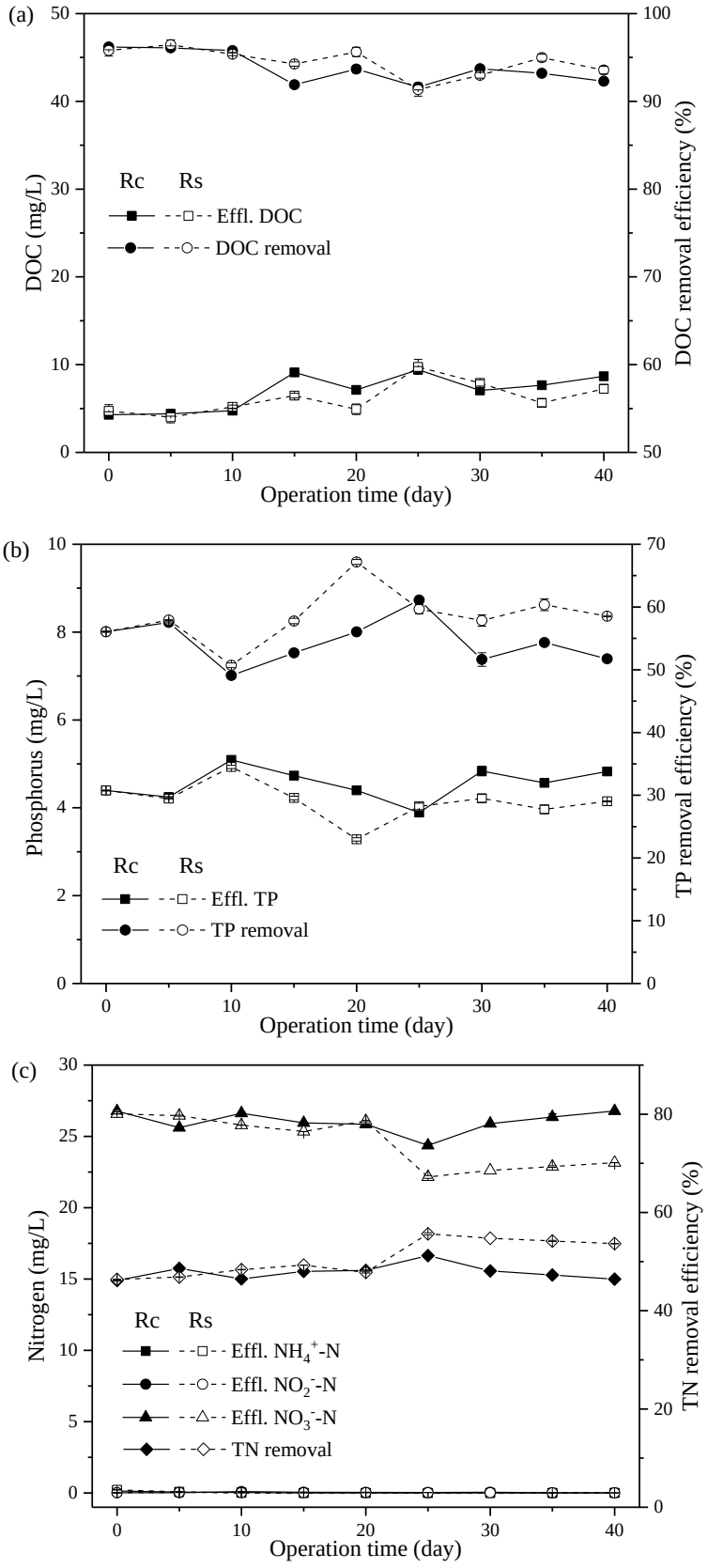

Figure 2-2 Variation of effluent dissolved organic carbon (DOC) and DOC removal efficiency (a), effluent PO_4^{3-}-P and TP removal efficiency (b), effluent N profile and TN removal efficiency (c) in Rc and Rs during the 40 days' operation.

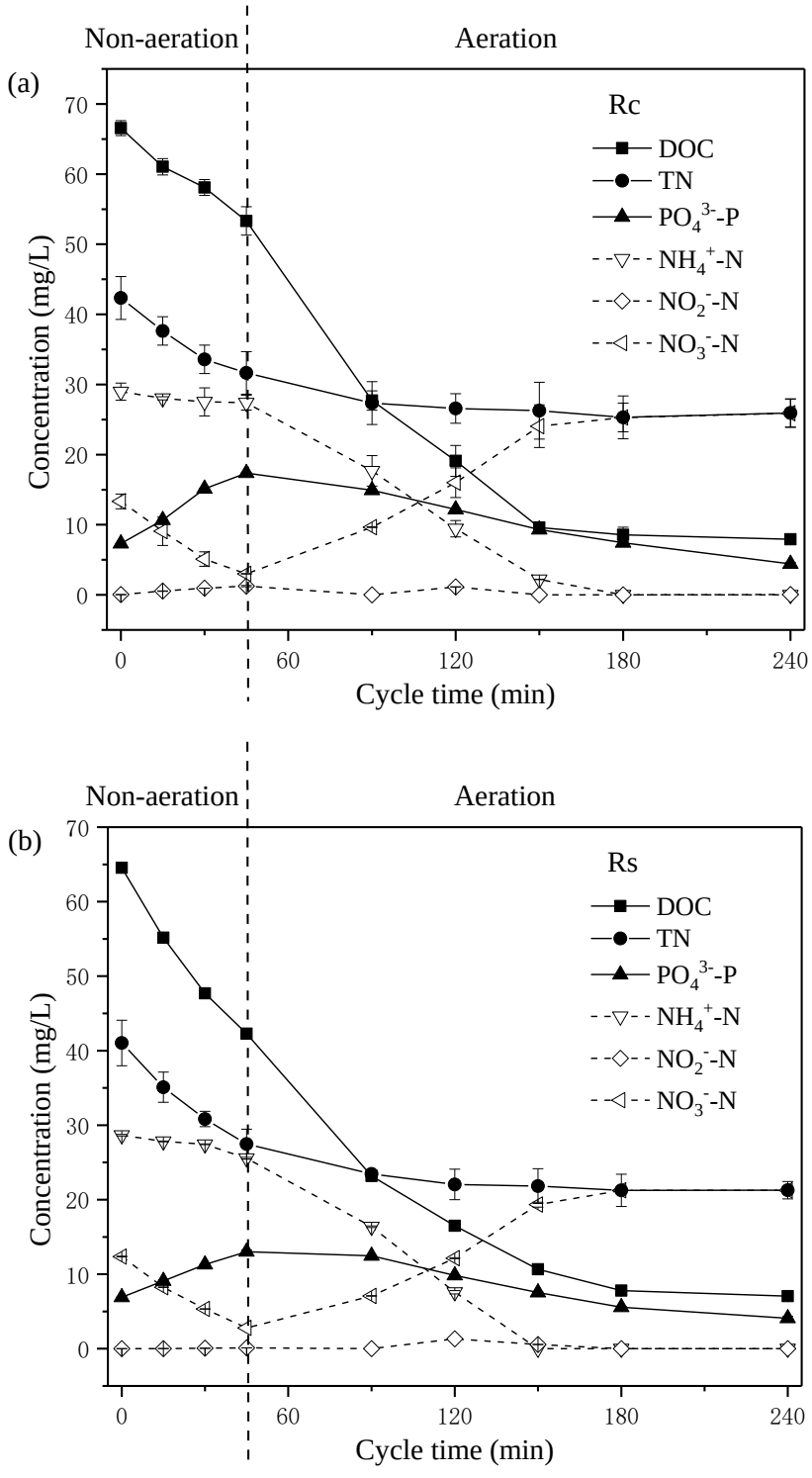

Figure 2-3 Variation of dissolved organic carbon (DOC), and effluent PO_4^{3-}-P, and N species in the typical cycles of Rc (a) and Rs (b) on day 32. Rc-the SBR without artificial sunlight, Rs-the SBR under artificial sunlight.

2.3.3 P fractionation in granules

The P fractionation in the granules from the two reactors were performed during the operation by using SMT method (Figure 2-4). As seen, the NAIP content gradually increased from the initial 23.9 mg/g-SS to 26.1 and 30.9 mg/g-SS, accounting for 71% and 70% of TP respectively in the granules from Rc and Rs on day 40. The more accumulation of NAIP in the granules from Rs might be explained by higher metal ions content in the algal-bacterial granules, especially Fe and Al (Table 2-2). On the other hand, the OP content in the granules from Rc varied within 5.0-5.9 mg/g-SS, while it obviously increased from the initial 5.9 mg/g-SS (17% of TP) to 9.5 mg/g-SS (22% of TP) in the granules from Rs on day 40. Similar observation could be found in Huang et al. (2015b), in which OP content was almost constant in nitrifying AGS. In addition, increase in OP content of the algal-bacterial granules was also observed during the granulation process of pure algae by Cai et al. (2019), probably due to P assimilation by the algae. The AP content in the granules from Rc showed some slight increase till the end of experiment, from the initial 5.0 mg/g-SS (14% of TP) to 5.5 mg/g-SS (15% of TP) on day 40. However, for the granules in Rs, the AP content was detected to decrease to 3.8 mg/g-SS (8.5% of TP) on day 40. In this study, the P bioavailability ((NAIP + OP)/TP) varied slightly from the initial 86% to 85% in the granules of Rc, which increased from initial 86% to 92% in the granules from Rs after 40 days' operation. Results from this study indicate that the alga-bacterial granules could keep much higher bioavailable P content (40.4 mg/g-SS, 92%), reflecting its great potential for P recovery.

2.3.4 Microbial and algal community analysis

The taxonomic affiliation of the dominant bacteria and algae in the granular consortia on day 40 is illustrated in Figure 2-5. In the Rc- and Rs- granules, Proteobacteria (75.1% and 67.2%) (including the Alpha-, Beta-, Delta-, and Gamma-proteobacteria) and Bacteroidetes (18.2% and 25.4%) (including the Sphingobacteriia and Flavobacteriia) were the dominant phyla on day 40, accounting for 93.3% and 92.8%, respectively. At the phylum level, Bacteroidetes and Proteobacteria are responsible for highly stable COD and NH_4^+-N removal capability (Cai et al., 2016; Zhong et al., 2016). The predominance of Proteobacteria in the granules from Rc and Rs in this study is consistent with the observations on both AS (Zhang et al., 2011) and AGS systems (Liao et al., 2013). At the class level, the Sphingobacteriia, accounting for 9.6% in the granules from Rc and 22.1% in those from Rs, including some filamentous bacteria, might contribute a lot to the granulation of algal-bacterial consortia through bridging with EPS (He et

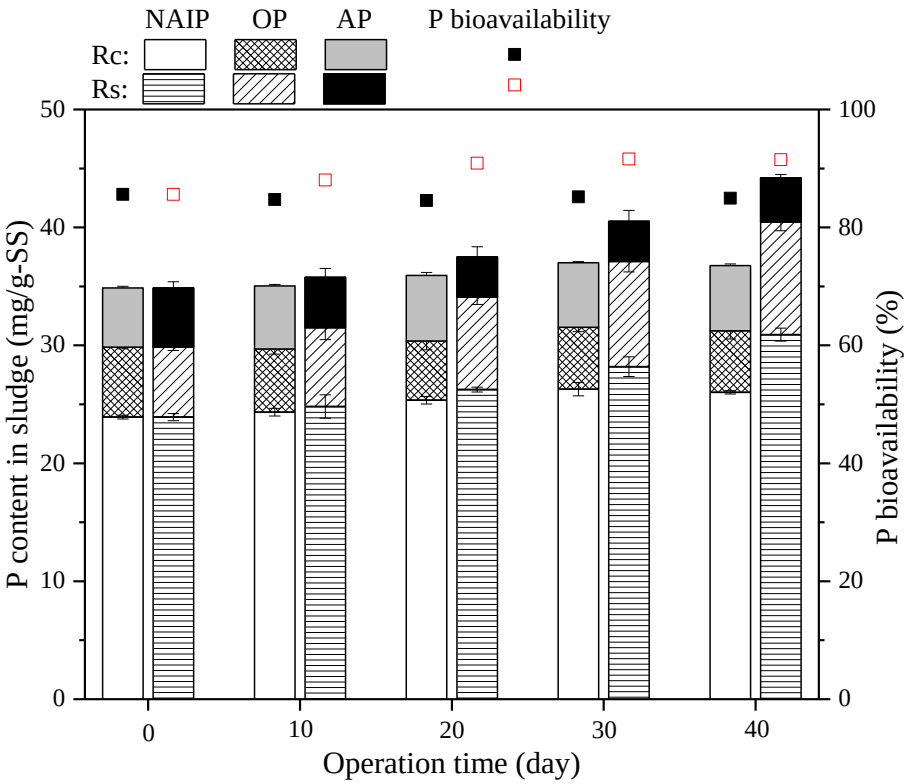

Figure 2-4 Variation of P fractionation and its bioavailability in the granules from Rc and Rs during the 40 days' operation. NAIP-non-apatite inorganic phosphorus, OP-organic phosphorus, AP-apatite phosphorus.

Table 2-2 Changes in average element contents in granules from Rc and Rs during 40 days' operation (unit: mg/g-SS).

Day	Sample	Na	K	Fe	Ca	Mg	Al
0	Initial	6.87	4.87	4.66	18.94	10.77	0.11
10	Rc-granules	7.34	5.76	5.67	17.44	7.85	0.22
	Rs-granules	7.41	4.39	5.94	19.70	18.03	0.24
20	Rc-granules	8.91	6.08	5.17	22.54	5.87	0.19
	Rs-granules	7.62	4.67	7.29	21.69	11.27	0.37
40	Rc-granules	9.88	5.17	6.74	15.98	9.65	0.31
	Rs-granules	8.15	7.26	13.46	18.67	13.16	0.99

Note: Rc-the SBR without artificial sunlight, Rs-the SBR under artificial sunlight.

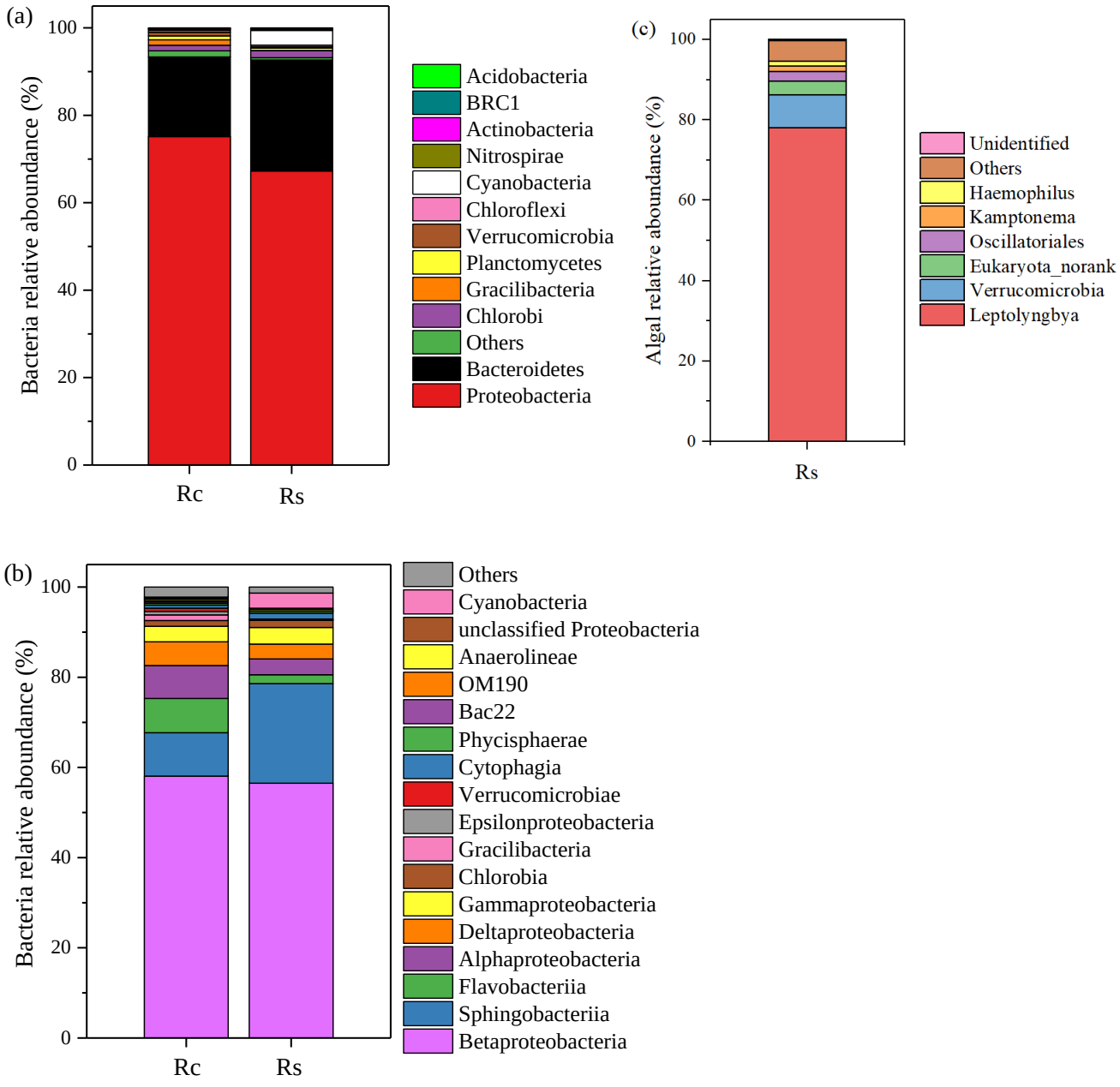

Figure 2-5 Taxonomic classification of the bacterial communities of the granules in Rc and Rs on day 40 at phylum level (a) and at class level (b), and taxonomic classification of the algal communities in the granules from Rs at genus level on day 40 (c). Rc-the SBR without artificial sunlight, Rs-the SBR under artificial sunlight.

al., 2018). Moreover, Meng et al. (2019) and Liu et al. (2018b) reported that the family of Sphingobacteriaceae (belonging to the class of Sphingobacteriia) is proposed as an oleaginous microorganism with the long chain fatty acids (C15 and C17), which could affect the biodiesel production from the granular sludge. As expected, more biodiesel might be obtained from the algal-bacterial granule due to the enriched Sphingobacteriia compared with the granules from Rc. Little difference could be found on the Betaproteobacteria and Gammaproteobacteria in the granules from Rc (58.1% and 3.5%) and in those from Rs (56.5% and 3.7%), which are important denitrifying bacteria and AOB according to Lim et al. (2005) and Adav et al. (2008). As for the algae, *Leptolyngbya*, occupying about 78.1%, was the most predominant algae species (Figure 2-5c). Seen from Shimura et al. (2015), this algae species is widely distributed throughout terrestrial environments and freshwater.

2.4 Summary

The algal-bacterial AGS system could be successfully developed by seeding bacterial AGS without algae inoculum under light illumination. The mature algal-bacterial granules exhibited a compact structure with high stability, large size, and good settling properties. Moreover, slightly higher TN (averagely 54.6%) and TP (averagely 58.4%) removal efficiencies were achieved in the algal-bacterial AGS system, in comparison to 48.3% and 54.5% respectively in the bacterial AGS system. More importantly, compared with the P content (36.8 mg/g-SS) and P bioavailability (85%) of the bacterial granules, higher P content (44.2 mg/g-SS) with higher P bioavailability (92%) was detected in the algal-bacterial granules, indicating its high potential for P recovery to serve multipurposes.

Chapter 3 Effect of low COD/N ratio on the granular stability, nutrients removal and accumulation of the algal-bacterial AGS

3.1 Introduction

Results from Chapter 2 demonstrated that the algal-bacterial granules could possess compact structure with high stability and higher bioavailable P content when treating domestic wastewater. In WWTPs, the carbon source in wastewaters becomes a key factor affecting the performance of nutrients removal. However, biodegradable carbon sources in wastewater are often reported to be insufficient in many areas worldwide, making it a big challenge to maintain desirable N and P removals. Therefore, the addition of external carbon source is usually required in order to meet the stringent effluent standards for WWTPs, resulting in increased treatment cost of WWTPs. In this study, the requirement of carbon source for nutrients removal might be reduced owing to the co-existence of algae in the symbiosis system. very little information is available regarding the influence of wastewater COD/N ratio on granular stability in the algal-bacterial AGS system, let alone the changes in nutrients removal and accumulation during the treatment of low COD/N wastewaters which always happens in municipal wastewater and/or its combination with industrial wastewaters.

This study aimed to investigate the effect of decrease in wastewater COD/N ratio (from 8 to 1) on the granular stability, nutrients removal and accumulation of the algal-bacterial AGS. The granules' morphology, strength and EPS content were observed and analyzed. In addition, nutrients (P and N) accumulation and P bioavailability in algal-bacterial granules were explored. Results from this work are expected to provide scientific reference and guidance for the operation and maintenance of this novel AGS system.

3.2 Materials and methods

3.2.1 Experimental set-up and operation conditions

As shown in Figure 3-1, two identical SBRs were operated under different influent COD/N ratios, i.e., R_1 (control, COD/N = 8) and R_2 (with COD/N varied from 8 to 4, 2, 1). Synthetic wastewater was used in this study and prepared with sodium acetate as the sole carbon source in the experiments. A stepwise decrease in influent COD/N ratio was applied to R_2 with less addition of sodium acetate (while keeping at a constant N concentration) during the operation. Its influent COD/N ratio varied from 8 to 4, 2, and 1, respectively when the influent COD concentration decreased from 400 to 50 mg/L during the four experimental stages (I, II, III, and

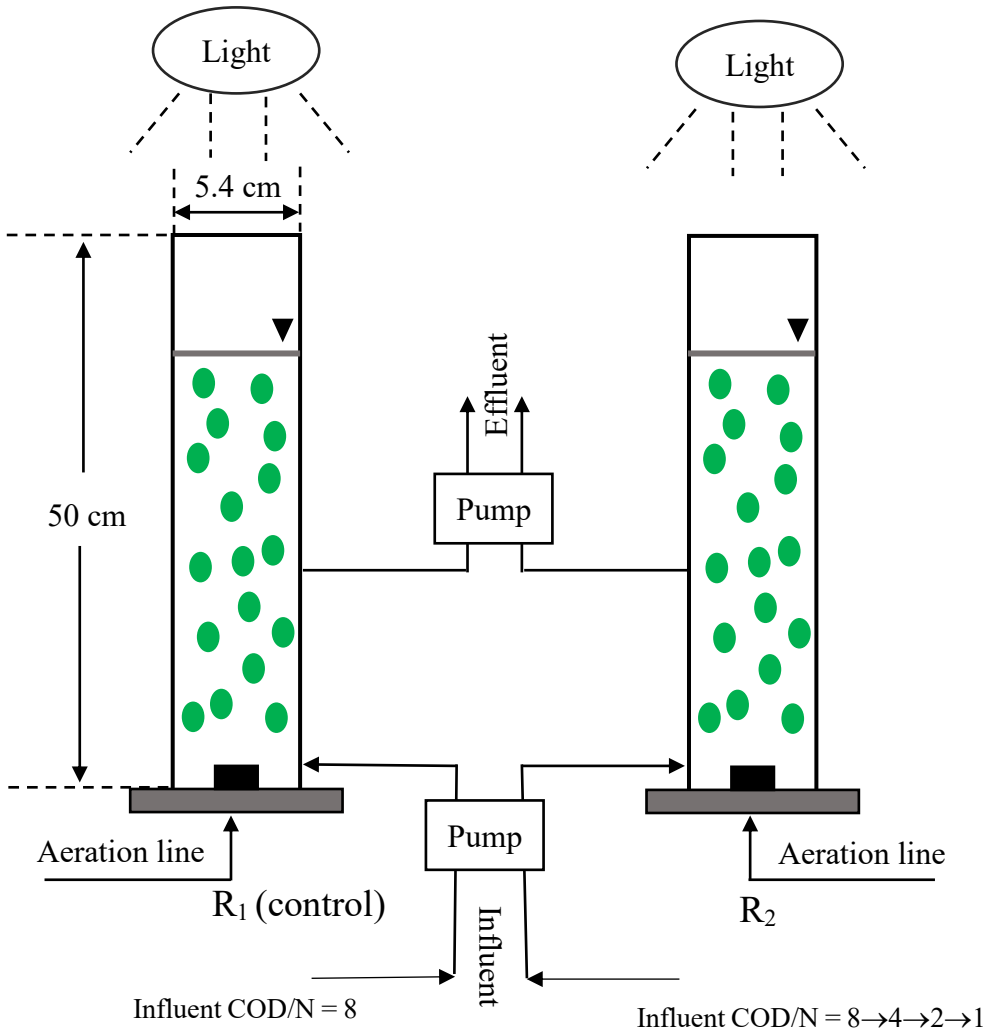

Figure 3-1 Structural diagram of the SBR systems used in this study.

Table 3-1 The influent COD/N ratios applied to the two reactors during different operation stages.

Stage	Day (start-end)	Influent COD/N ratio	
		R_1	R_2
I	0-20	COD (400 mg/L): N (50 mg/L) = 8:1	COD (400 mg/L): N (50 mg/L) = 8:1
II	21-40		COD (200 mg/L): N (50 mg/L) = 4:1
III	41-65		COD (100 mg/L): N (50 mg/L) = 2:1
IV	66-90		COD (50 mg/L): N (50 mg/L) = 1:1

Note: COD-chemical oxygen demand, R_1-influent with constant COD/N = 8, R_2-influent with stepwise decrease of COD/N from 8 to 1.

IV) (Table 3-1). Other nutrients were added into the influent at the same levels throughout the experiments, including 50 mg NH_4^+-N/L (NH_4Cl), 10 mg PO_4^{3-}-P/L (KH_2PO_4), 10 mg Ca^{2+}/L ($CaCl_2$), 5 mg Mg^{2+}/L ($MgSO_4 \cdot 7H_2O$), 5 mg Fe^{2+}/L ($FeSO_4 \cdot 7H_2O$), and 1 mL/L of trace elements solution. The influent pH was adjusted to 7.5-7.7 by adding 300 mg/L of $NaHCO_3$ in the influent. Light illumination condition tested in this study is same with the Chapter 2.

The two reactors were operated at room temperature (25 ± 2°C) for 90 days under alternatively anaerobic and aerobic conditions with each cycle of 4 h. Each cycle consisted of 2 min filling, 60 min non-aeration period, 173 min aeration period, 2 min settling, and 3 min effluent discharge. During aeration, air was provided by an air pump (AK-40, KOSHIN, Japan) from the bottom of reactor through air bubble diffusers at an air flow rate of 0.55 cm/s. Other parameters including HRT and SRT are accordance with section 2.2.1 in Chapter 2.

3.2.2 Analytical methods

Effluent DOC, dissolved inorganic carbon (DIC), and dissolved total carbon (DTC) were measured by the TOC analyzer (TOC-V_{CSN}, SHIMADZU, Japan) equipped with an auto-sampler (ASI-V, SHIMADZU, Japan).

Loosely bound EPS (LB-EPS) was extracted using the method described by Miao et al. (2016) with slight modifications. Briefly, 5 mL sample was centrifuged at 5000 *g* for 15 min. The supernatant was filtered through 0.22 μm membrane, and the filtrate was collected to represent the LB-EPS fraction. Tightly bound EPS (TB-EPS) extraction procedure was carried out according to the method described by Adav and Lee (2008) with some modifications. After the supernatant being discarded for the measurement of LB-EPS, the residual sludge was resuspended with 0.9% (w/v) NaCl to the original volume, and then heated to 80℃ and kept at this temperature for 30 min. The extracted solution was centrifuged at 10000 *g* for 20 min under 4℃, then the supernatant was filtrated through 0.22 μm membrane and the collected filtrate was used for analysis of the TB-EPS fraction. The EPS samples (both LB- and TB-EPS) were stored at -30℃ prior to analysis. Extracellular polysaccharides (PS) and proteins (PN) in the extracted EPS were measured by using the phenol-sulfuric acid method and the Lowry-Folin method, respectively (Herbert et al., 1971; Lowry et al., 1951).

The other analytical methods have been described in section 2.2.2.

3.3 Results and discussion

3.3.1 Characteristics of algal-bacterial AGS during 90 days' operation

(1) Granular morphology

Initially, the mature granules were green in most parts of the granules, which reflected an irregular shape, compact and dense structure (Figure 3-2). After day 30, almost all the granules in R_1 and R_2 turned into dark green till the end of experiment, probably due to some changes of algal species exposed to lower light illuminance as the quantity and size of granules increased. On day 90, the granules in the two reactors kept their compact and dense structure, and the granules in R_2 were relatively smaller compared to those in R_1.

(2) Granule growth and its size distribution

The changes in granular size and its distribution in R_1 and R_2 are shown in Figure 3-3. At the beginning, the granules were mainly within 1.0-1.5 and 1.5-2.0 mm, occupying about 46% and 46% of the total granules in both reactors, respectively. After 90 days' operation, larger particles dominated in both reactors, but the granular size distribution was obviously different between the granules from these two reactors. The granules ranging within 2.0-2.5 mm and > 2.5 mm accounted for 29% and 63% in R_1, respectively. In contrast, the granules of 2.0-2.5 mm gradually became the dominant portion in R_2 (about 48% on day 90). Figure 3-3 also shows the average diameter of granules in the two reactors. On day 90, the average granular size in both reactors was averagely increased from the initial 1.54 ± 0.29 to 2.62 ± 0.53 mm (R_1) and 2.33 ± 0.51 mm (R_2), respectively. This phenomenon is mainly attributable to the difference in organic loading to these two reactors. As stated, a higher COD loading would generally result in bigger granules with a compact structure (Liu et al. 2003). Results from this work show that the decrease in influent COD/N ratio exerted some influence on the granular size and its distribution as well.

(3) Biomass increase, sludge settleability and granular stability

Figure 3-4 demonstrates the changes in MLSS and MLVSS/MLSS ratio of granules in the two reactors. The initial algal-bacterial AGS MLSS was 5.25 g/L in R_1 and 5.30 g/L in R_2 with the same MLVSS/MLSS ratio of 0.78. From day 21 (Stage II) on, the MLSS in R_2 dropped sharply, and finally tended to be stable during Stage IV, which was basically maintained around 3.21 g/L. This phenomenon, i.e. a lower biomass growth in R_2, was probably attributable to the decrease in influent COD concentration from 400 to 50 mg/L. In contrast, the biomass in R_1 kept fluctuating at 5.92-7.63 g/L from day 28 to day 90, with the MLVSS/MLSS ratio of 0.76-0.79 during the experiment. While in R_2, the MLVSS/MLSS ratio of the granules fluctuated

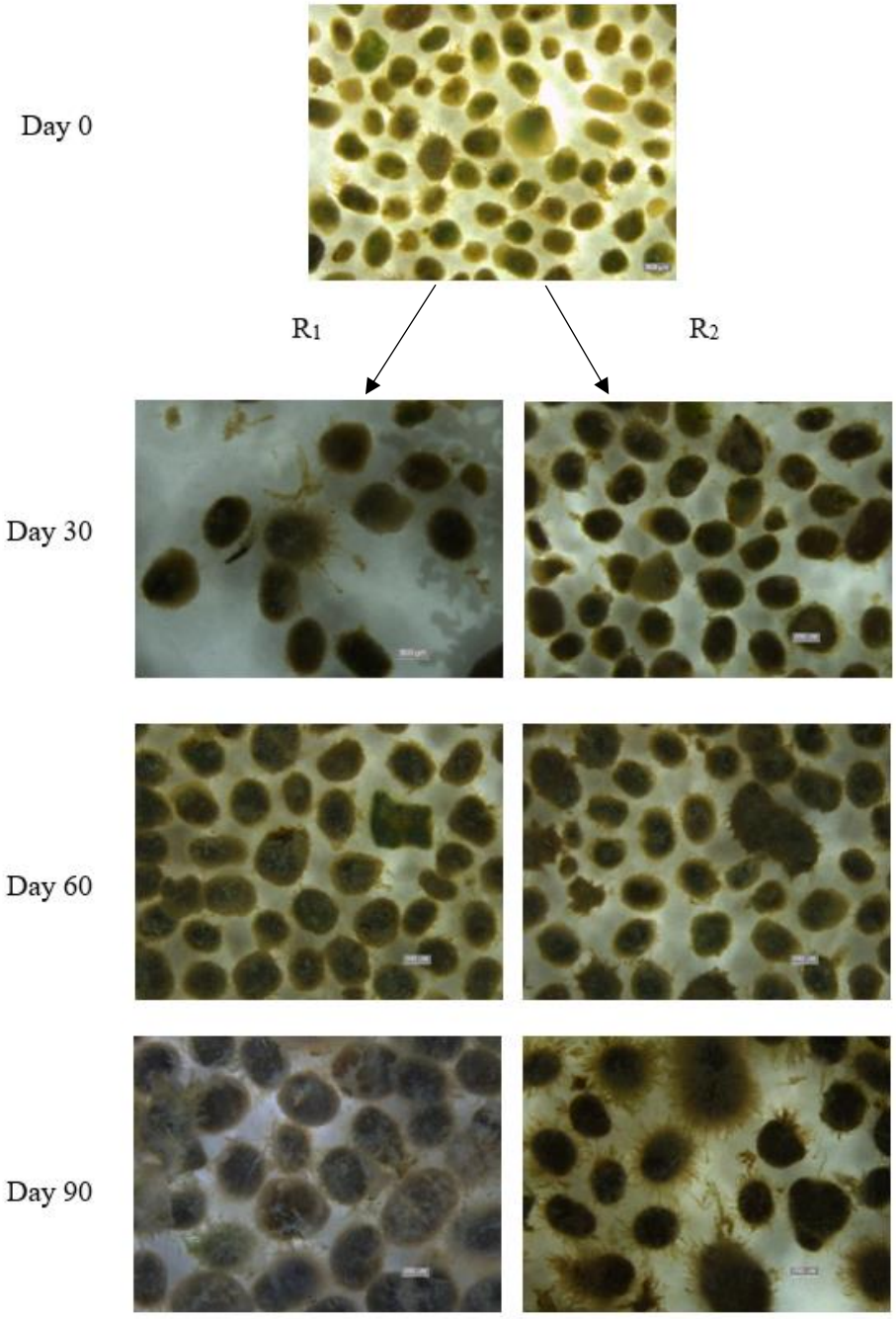

Figure 3-2 Morphological changes of the algal-bacterial AGS in the two reactors on day 0, 30, 60, and 90, respectively. R_1-influent with constant COD/N = 8, R_2-influent with stepwise decrease of COD/N from 8 to 1.

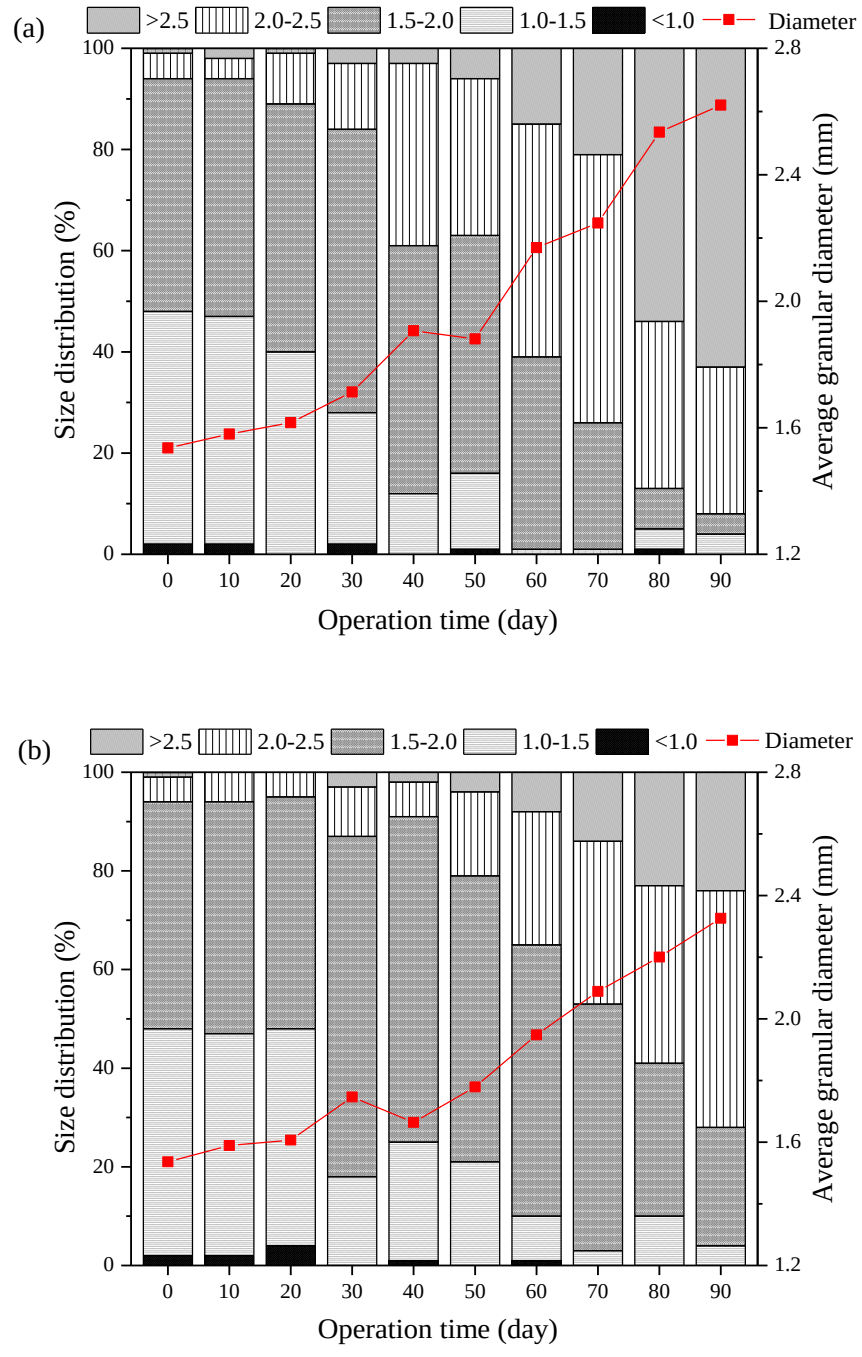

Figure 3-3 Dynamic changes of algal-bacterial AGS diameter and its size distribution in R_1 (a) and R_2 (b). R_1-influent with constant COD/N = 8, R_2-influent with stepwise decrease of COD/N from 8 to 1.

between 0.75-0.79 before Stage III, which was slightly decreased to 0.70-0.72 during Stage IV (at influent COD/N ratio = 1). This observation indicates that the growth of biomass in the algal-bacterial granular system is dependent on the influent organics or carbonaceous substances to some extent, while this system can also quickly adapt to the low carbon environment like COD/N = 1. On the other hand, a relatively low MLVSS/MLSS ratio for the granules in R_2 during Stage IV (COD/N = 1, Figure 3-4a) might imply that more mineral substances (especially Fe) were accumulated into the granules under this operation condition (Oehmen et al., 2007).

SVI and settling velocity can be used to indicate the settleability of granular sludge. Figure 3-4b shows the changes in SVI_5 and settling velocity of the granules from the two reactors. The granular SVI_5 values were determined to vary between 33.1-47.7 mL/g in R_1, signaling the good settleability of algal-bacterial granules during the long-term operation. This observation is in accordance with the results from Ni et al. (2009) who found that SVI_{10} and SVI_{30} values were stably below 50 mL/g when feeding low-strength municipal wastewater into AGS reactors. In R_2, the SVI_5 fluctuated between 34.2-44.7 mL/g till day 70 and increased to 61.5 and 58.1 mL/g on day 84 and day 90, respectively. A much lower MLSS concentration in R_2 during Stage IV (Figure 3-4a) to some extent contributed to the increase in SVI_5 of its granules. For the granular sludge in R_1 and R_2, the settling velocity was detected to averagely decrease from the initial 32.0 to 27.6 and 15.0 m/h respectively at the end of operation. The above results show that the low carbon influent might limit the growth of fast-settling bacteria in the algal-bacterial AGS, possibly resulting in the much lower MLVSS or MLSS concentration in R_2, especially during Stages III and IV. In addition, some filamentous bacteria were observed to grow in the two reactors till the end of experiment, which seemed to have some negative effect on the settleability of algal-bacterial AGS.

In this study, granular stability was expressed in terms of integrity coefficient, and a lower value denotes a better stability (Muda et al., 2010). As shown in Figure 3-4c, the integrity coefficient of the granules in R_1 was between 0.9-2.2% during the 90 days' operation, signaling the excellent stability of algal-bacterial AGS. However, the integrity coefficient of the granules in R_2 increased from 0.7 to 5.4% when the influent COD/N ratio decreased from 8 to 1, implying that the low carbon influent (COD/N = 4, 2 and 1) exerted some negative effect on the stability of granules. However, according to Ghangrekar et al. (2005), granules with integrity coefficient of less than 20% were considered as high-strength granules. Therefore, it is worthwhile to note

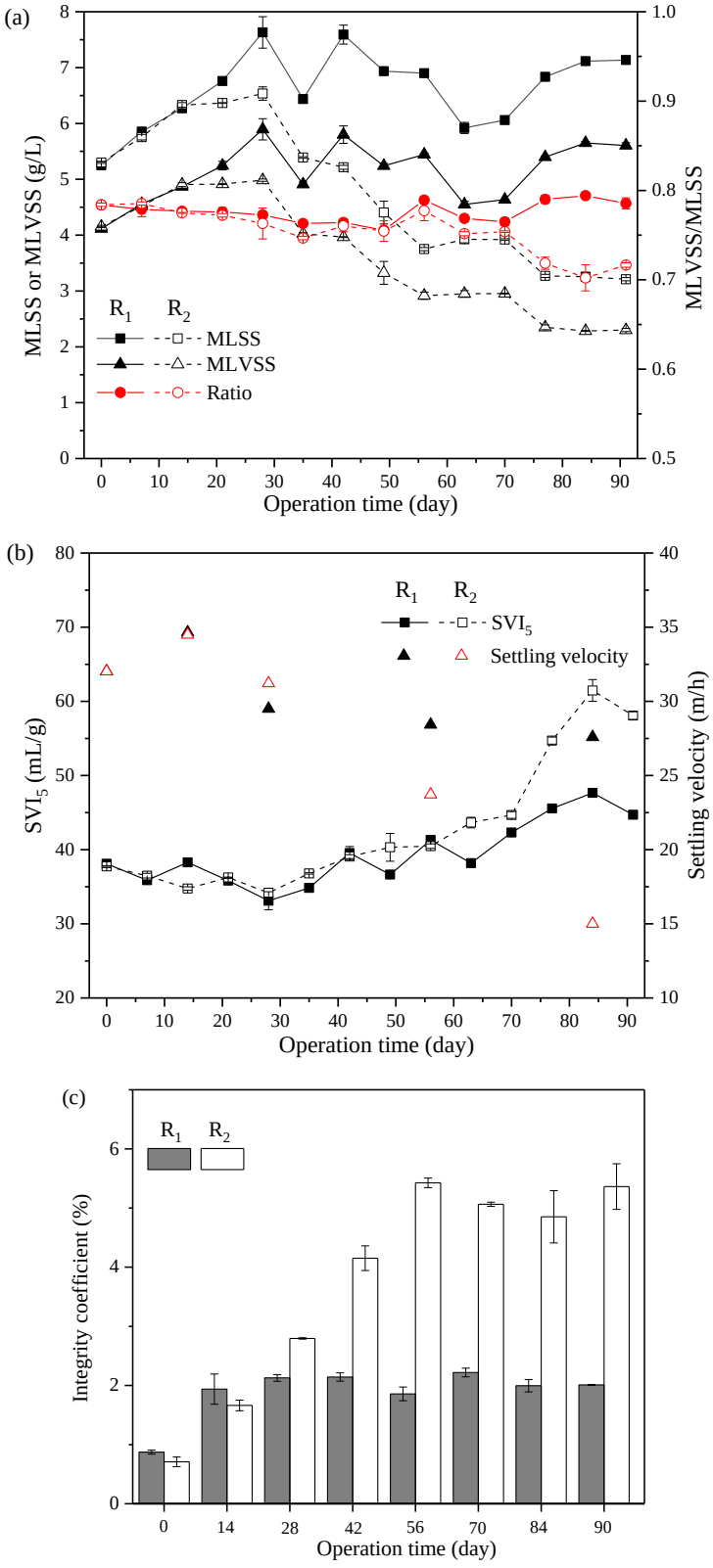

Figure 3-4 Characteristics of algal-bacterial AGS in R_1 and R_2 during the 90 days' operation: ML(V)SS and MLVSS/MLSS ratio (a), SVI_5 and settling velocity (b) and integrity coefficient (c). R_1-influent with constant COD/N = 8, R_2-influent with stepwise decrease of COD/N from 8 to 1.

that the algal-bacterial AGS possesses excellent granular stability and integrity, even being applied to treat low carbon wastewater (COD/N = 1). In addition, the whole system could quickly adjust and positively respond to the decrease in influent carbon concentration. This observation is different from Luo et al. (2014) and Kocaturk and Erguder (2016) who noticed the occurrence of aerobic granule disintegration when the influent COD/N ratio decreased to 1, which might be associated with the different influent characteristics and co-existing algae in the algal-bacterial AGS system in this study.

3.3.2 Reactor performance

(1) Carbon removal

The changes in effluent DOC concentration and removal efficiency in R_1 and R_2 are shown in Figure 3-5. During the whole experimental period, the DOC removal efficiency was averagely 96% in R_1 with effluent DOC being always < 11 mg/L, signaling the excellent organics removal of the algal-bacterial AGS system. When the influent COD was decreased to 200 mg/L (COD/N = 4) from day 20 on, interestingly, little difference in DOC removal efficiency was noticed in R_2, around 95-96%; while some decrease in DOC removal efficiency was discerned, averagely 90.6 or 82.5% when the influent COD concentration was further decreased to 100 or 50 mg/L (COD/N = 2 or 1) as scheduled. However, importantly, in comparison to the effluent from R_1 (averagely 6 mg/L), a lower DOC concentration (averagely 4 mg/L) was always detected in the effluent from R_2 throughout the whole experiment. This observation indicates that the algal-bacterial AGS system can be used to treat varying strength of organic wastewater.

Figure 3-5b presents the changes in DTC and DIC concentrations in the effluents from the two reactors during the operation. Compared with the relatively stable DIC concentration (45-55 mg/L) in the effluent from R_1, the DIC concentration in the effluent from R_2 was significantly decreased from averagely 52 to 10, 2, and 1 mg/L when the influent COD concentration was adjusted from 400 to 200, 100, and 50 mg/L, respectively. This phenomenon may be attributable to the growth of algae who were responsible for the enhanced DIC uptake since much more increase in chlorophyll *a* concentration was detected in the granules from R_2 along with the operation by feeding low COD/N ratio wastewater. This observation also implies that the algal-bacterial AGS system could be very promising for reduction in greenhouse gases (GHGs) emission from wastewater treatment. Further research is necessary for optimization of the operation conditions and quantification of GHGs emission reduction.

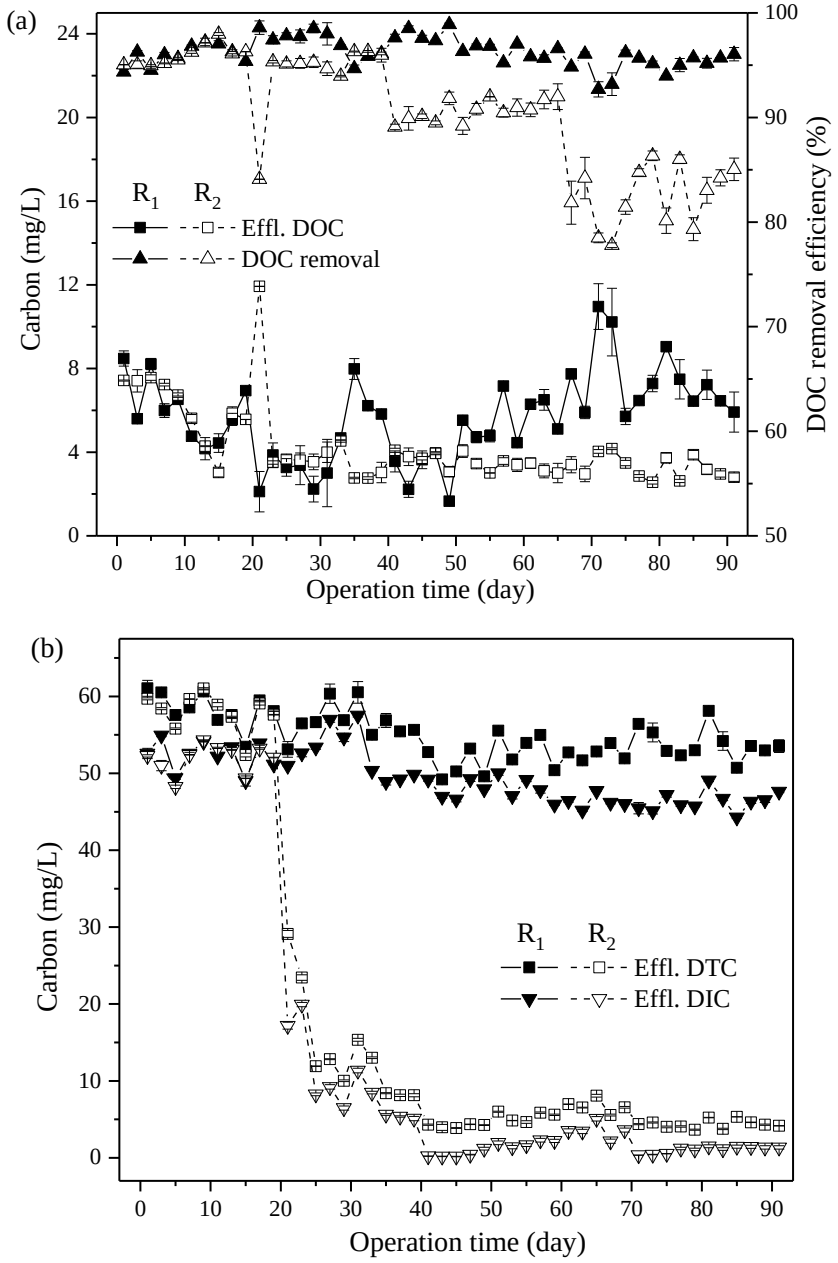

Figure 3-5 Variation of effluent DOC concentration and DOC removal efficiencies (a), effluent DIC and DTC concentrations (b) in R_1 and R_2 during the 90 days' operation. R_1-influent with constant COD/N = 8, R_2-influent with stepwise decrease of COD/N from 8 to 1.

(2) Nitrogen and phosphorus removal

In order to investigate the effect of influent COD/N ratio on nitrification in the algal-bacterial AGS system, N species including NH_4^+-N, NO_2^--N, and NO_3^--N were monitored in the two reactors when the stepwise decrease in influent COD from 400 to 50 mg/L was applied to R_2. The changes in N concentrations in the effluents from both reactors are shown in Figure 3-6. Correspondingly, their nitritation and nitratation efficiencies calculated according to Li et al. (2015) are depicted in Figure 3-6b. It is clearly that the two reactors exhibited excellent nitratation efficiency (97-100%). That is, in both systems NO_2^--N can be easily converted into NO_3^--N under the designed operation conditions. In addition, little NO_2^--N (less than 1.4 mg/L) was detected in the effluents from both reactors till the end of experiment. These results imply that the decrease in influent COD/N ratio from 8 to 1 seems to have little influence on nitratation process of the algal-bacterial AGS system. When the influent COD/N ratio decreased to 2 in R_2 during Stage III, however, a clear difference was noticed in nitritation efficiency between R_1 and R_2: higher effluent NH_4^+-N concentrations and thus lower nitritation efficiency were detected in R_2 (averagely 5.7 mg/L and 88%) than R_1 (~ 0 mg/L and 100%). The effluent NH_4^+-N concentration from R_2 increased sharply from day 65 (Stage IV, COD/N = 1), and the nitritation efficiency dropped promptly to lower than 70% (averagely 69%). On the other hand, simultaneous denitrification occurred during the whole operation, which was greater at higher influent COD/N ratio conditions according to the NO_3^--N and TN removal results. Therefore, it can be inferred that lower influent COD/N ratio (4, 2 and 1) might negatively impact the nitritation and denitrification processes in the algal-bacterial AGS system. The SOUR, SNUR, and SAUR of the granules from R_1 and R_2 were also measured (Table 3-2). The granules from R_1 exhibited almost similar or slightly enhanced bioactivities in terms of SOUR, SAUR and SNUR during the whole experiment. The SOUR of granules from R_2, however, decreased from 24.5 to 9.1 mg O_2/g-VSS·h when the influent COD/N ratio was decreased from 8 to 1. On the other hand, the SAUR of granules from R_2 gradually decreased from 6.03 to 3.42 mg N/g-VSS·h along with the operation; while little change in SNUR was detected in the granules from R_2 during the test period. The changes in granular SAUR and SNUR are in accordance with the variations in the effluent N concentrations detected and the two reactors' nitritation and nitratation efficiencies (Figures 3-5a and b). Two reasons might be contributed to the lower SOUR and SAUR of granules from R_2: (1) The ammonia-oxidizing bacteria and heterotrophic bacteria in the algal-bacterial AGS may have lower microbial activities; and (2) the ammonia uptake by algae might be inhibited when feeding low COD/N ratio wastewaters. In the

meantime, the sharp decrease in TN removal capacity in R_2 (Figure 3-6c) implies that denitrification by heterotrophic bacteria contributed more to the TN removal in the algal-bacterial AGS system compared to the N assimilation by the grown algae that increased remarkably under the tested conditions. The detailed mechanisms still need further investigation.

Figure 3-6c also shows the average TP removal capacity during the 90 days' operation. The two reactors exhibited almost a similar variation trend during the whole operation, ranging between 1.9-5.5 mg/g-VSS·d (R_1) and 1.9-5.4 mg/g-VSS·d (R_2), respectively. This observation might be attributable to the application of the same SRT (30 days) to control both reactors. A slightly higher average TP removal capacity was detected in the granules from R_1 (averagely 4.1 mg/g-VSS·d) than those from R_2 (3.6 mg/g-VSS·d), possibly owing to the difference in biomass concentrations in the two reactors (Figure 3-4a). However, at the end of the experiment, the TP removal capacity was almost same in both reactors (~ 3.5 mg/g-VSS·d), indicating that influent COD/N ratio might have little influence on TP removal capacity in the algal-bacterial AGS system, which is probably controlled by SRT. On the other hand, during the operation the anaerobic P release and aerobic P uptake rates were also determined in the two SBRs on days 10, 30, 55, and 85, respectively. As shown, the average anaerobic P release and aerobic P uptake in R_2 decreased from the 6.07 and 2.33 mg/g-VSS·h on day 10 to 0.21 and 0.09 mg/g-VSS·h on day 85, suggesting the growth or activity of PAOs in R_2 might be inhibited under low influent COD/N ratio conditions. This observation may contribute to the slight decrease in P removal capacity in R_2 (Figure 3-6c) to some extent. As it is known, P can be removed from wastewater through both biotic P assimilation into the biomass and abiotic P precipitation (de Godos et al., 2009). In case of the algal-bacteria AGS system in this study, most probably co-precipitation of phosphate with other co-existing metals (Huang et al., 2015b) and algae assimilation were the major contributors to the relatively stable P removal (Figure 3-6c) in R_2 under the low influent COD/N ratio conditions. Since only 1-15% of the anaerobic bacterial P release and aerobic bacterial P uptake (typically for PAOs) rates were detected in the granules from R_2, optimization of the operation conditions or strategies is crucial for enhanced P removal and accumulation by using this algal-bacterial AGS system.

3.3.3 Variation in nutrients content in the granules during the operation

The TP content analysis and P fractionation in the granules from the two reactors were performed during the operation by using SMT method (Figure 3-7). In general, The TP content in the granules reflected a similar trend in the two reactors and reached to 30.8 and 30.6 mg/g-

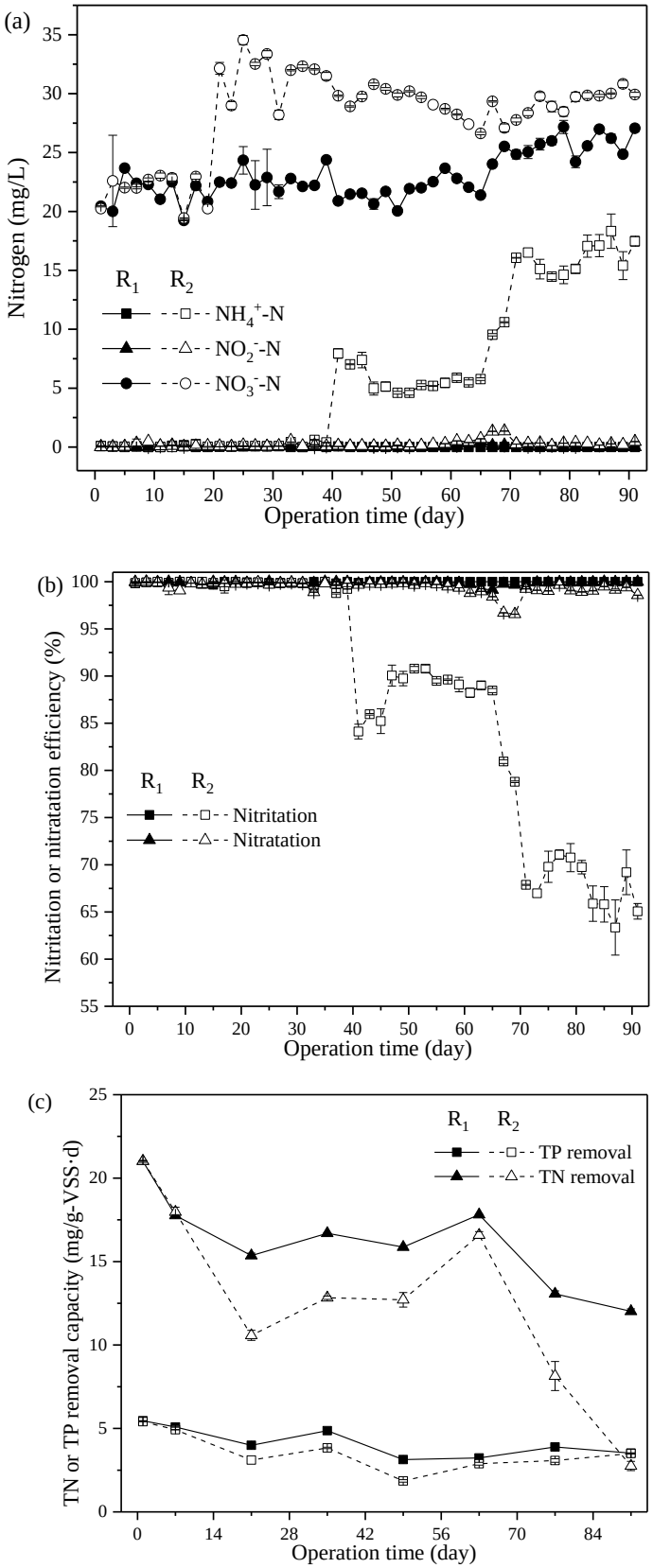

Figure 3-6 Variation of effluent N (NH_4^+-N, NO_2^--N, and NO_3^--N) concentrations (a), nitritation and nitratation efficiencies (b), and TN and TP removal capacities (c) by R_1 and R_2 during the 90 days' operation.

Table 3-2 Variations of the average specific oxygen utilization rate (SOUR), specific ammonia uptake rate (SAUR), specific nitrite uptake rate (SNUR), anaerobic P release and aerobic P uptake rates of granules from the reactors during the 90 days' operation.

Day*	SAUR (mg-N/g-VSS· h)		SNUR (mg-N/g-VSS· h)		SOUR (mg-O_2/g-VSS· h)		Anaerobic P release rate (mg-P/g-VSS· h)		Aerobic P uptake rate (mg-P/g-VSS· h)	
	R_1	R_2	R_1	R_2	R_1	R_2	R_1	R_2	R_1	R_2
15	6.18	6.03	1.85	1.90	23.3	24.5	5.89	6.07	2.28	2.33
32	6.96	4.14	1.94	1.73	21.0	16.2	5.80	0.85	2.17	0.34
58	7.50	2.41	2.01	1.89	19.4	12.4	6.23	0.04	2.57	0.03
86	8.90	3.42	2.07	1.88	20.6	9.1	7.45	0.21	3.21	0.09

Note: * The determination of P release and uptake was conducted on day 10, 30, 55 and 85, respectively. R_1-influent with constant COD/N = 8, R_2-influent with stepwise decrease of COD/N from 8 to 1.

SS from R_1 and R_2, respectively on day 14 (Stage I). Specifically, during the operation of Stage II and Stage III (from day 28 to day 70, the influent COD/N ratio = 4 and 2, respectively), the TP content in the granules from R_2 was always a little bit lower than that from R_1, which then increased faster and thereafter higher than that from R_1 after day 84 (influent COD/N = 1). This observation is possibly associated with the P assimilation potential of algae which grew faster during Stage IV, as much higher amount of chlorophyll *a* in the granules from R_2 (13.0 mg Chl-a/g-VSS on day 84) was detected compared with that from R_1 (6.2 mg Chl-a/g-VSS on day 84) (Figure 3-8). On day 90, averagely 26.7 and 28.3 mg/g-SS of TP were respectively detected in the granules from R_1 and R_2. Future research work is still necessary for detailed information about the influence of algae growth on the P accumulation during the long-term operation of the algal-bacterial AGS system and its optimization.

Figure 3-7a also shows the changes in P fractionation (OP, IP (NAIP and AP)) during the operation. As seen, IP was the dominant P fraction in the seeded algal-bacterial AGS, occupying 76% and 75% of TP in the granules from R_1 and R_2, respectively. Both granules contained NAIP about 70% of TP. Besides, the NAIP content slightly decreased to 19.0 and 17.3 mg/g-SS, accounting for 75% and 62% of TP respectively in the granules from R_1 and R_2 on day 90. Interestingly, the OP content in the granules from R_1 decreased gradually till the end of experiment, about 4.5 mg/g-SS on day 90. In contrast, the OP content in the granules from R_2 gently varied between 5.5-6.7 mg/g-SS during Stage II and Stage III (from day 28 to day 70), which significantly increased to 8.1 and 10.1 mg/g-SS on day 84 and day 90, respectively. Most importantly, AP, the P form directly associated with Ca, was very low in the seeded granules, occupying only 5-6% of TP. Along with the operation from Stage II to Stage IV (day 28 to day 90), the AP content in the granules from R_2 decreased from 1.7 mg/g-SS (6% of TP) to 0.6 mg/g-SS (2% of TP), while it kept stable for the granules in R_1 (about 7% of TP on day 28 and day 90).

In addition, NAIP and OP can be used to indicate the potentially releasable and bioavailable P fractions (Pardo et al., 2003; Xie et al., 2011). The P bioavailability ((NAIP + OP)/TP) varied slightly from the initial 95% to 92% in the granules of R_1, which increased from initial 94% to 98% in the granules from R_2 after 90 days' operation. As reported, the proportion of (NAIP + OP) to TP was about 80% for AS and general AGS (Huang et al., 2015b). Results from this study indicate that the algal-bacterial AGS possesses high potential for P recovery from wastewater, resulting in P-rich granules with high P mobility and bioavailability. Moreover, much higher P bioavailability in granules was achieved in this study when the influent COD/N

ratio decreased to 1, suggesting some promotion mechanism of bioavailable P accumulation was stimulated under the extremely low carbon condition. This observation also indicates the great potential of using algal-bacterial AGS to recover P from wastewater, especially under low carbon conditions, and the resultant P-rich granules can be easily used for multiple purposes.

The TN content in the granules from the two reactors was also monitored during the whole operation (Figure 3-7b). As a result, little difference in TN content was detected in the granules from R_1 and R_2 during Stage I and Stage II, varying between 90-93 mg/g-SS. And a slight increase in TN content was detected in the granules from R_1, about 95 mg/g-SS at the end of experiment. However, from Stage III to Stage IV (day 42 to day 90), the TN content in the granules from R_2 remarkably decreased, about 70 mg/g-SS on day 90. Taking the increased effluent NH_4^+-N concentration (Figure 3-6a) together with the variation in TN content in the granules (Figure 3-7b) from R_2, it is speculated that some nitrogenous organics stored or entrapped in the granule matrix might be utilized as carbon source by heterotrophic microbes under the lower influent COD/N ratio conditions. If it happens, these organics might be decomposed into NH_4^+, to some extent resulting in the increase of effluent NH_4^+-N concentration. The real reason for the decreased TN removal at extreme low influent COD/N needs further detailed investigation.

3.3.4 Characteristic change of EPS content and its relationship with granular stability

The changes in PN, PS and the total EPS during the operation are shown in Figure 3-9. Clearly, the total EPS content in the granules from R_1 kept increasing till the end of experiment, from the initial 196.2 to 272.8 mg/g-VSS on day 90. However, for R_2, the EPS content in the granules was detected to increase in an almost same trend as that in R_1 before day 42 (the beginning of Stage III when the influent COD/N ratio was decreased from 4 to 2), then sharply and further decreased to about 114.5 mg/g-VSS on day 84. On day 90, it was slightly recovered to 122.6 mg/g-VSS. More specifically, the PS content in the granules increased gradually from the initial 18.0 mg/g-VSS to 39.1 and 51.9 mg/g-VSS on day 90 in R_1 and R_2, respectively, in which the granules from R_2 always had a higher PS content from the beginning of deceasing the influent COD/N ratio. On the other hand, when the influent COD/N ratio was decreased to 2 or 1, a remarkable reduction in PN content was noticed in the granules from R_2. Beun et al. (2002) pointed out that the typical range of PN/PS ratio in the aerobic granules was 0.1-5. In this study, although the PN/PS ratios in the granules from both reactors obviously decreased due to the reduction of PN content or increase in PS content in granules, the PN/PS values were

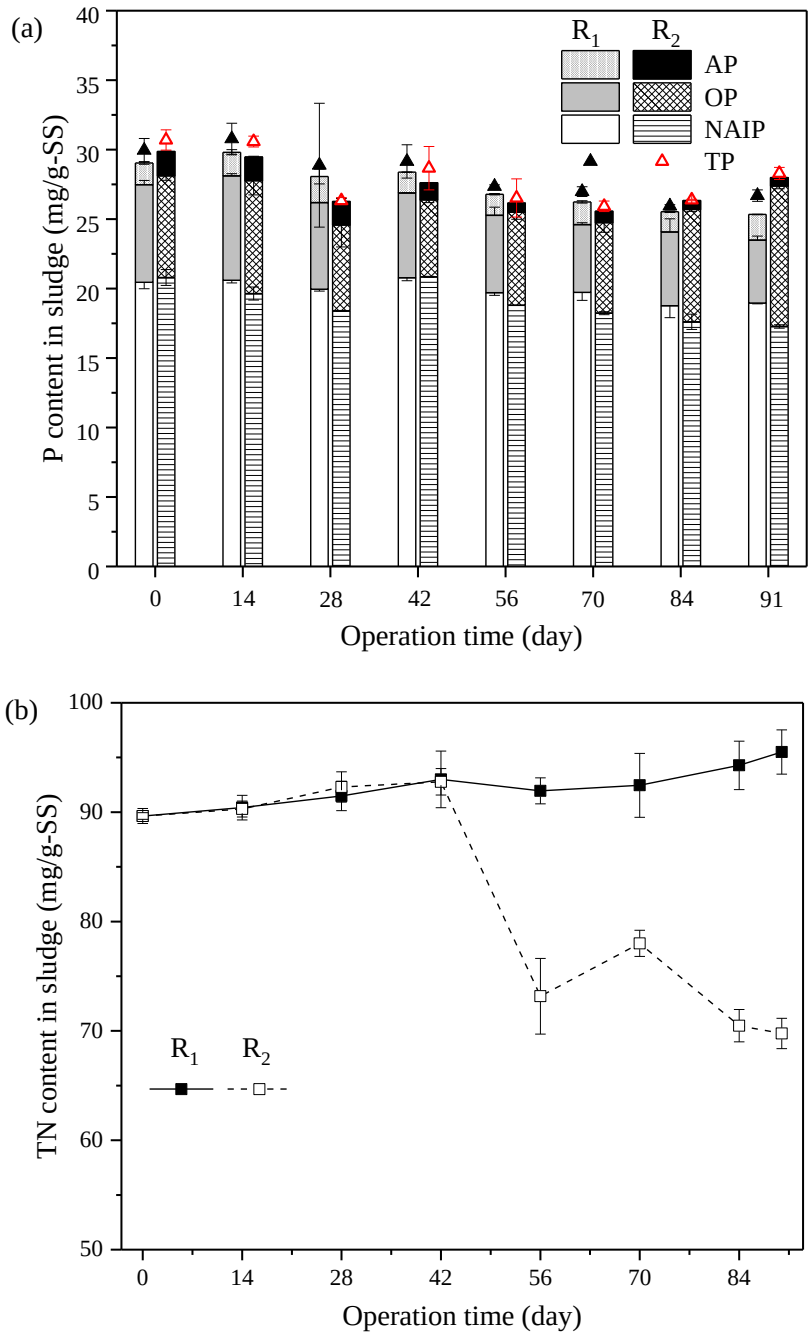

Figure 3-7 Variations of P content and fractionation (a), and TN content (b) in the granules from R_1 and R_2 during the 90 days' operation. R_1-influent with constant COD/N = 8, R_2-influent with stepwise decrease of COD/N from 8 to 1. NAIP-non-apatite inorganic phosphorus, OP-organic phosphorus, AP-apatite phosphorus.

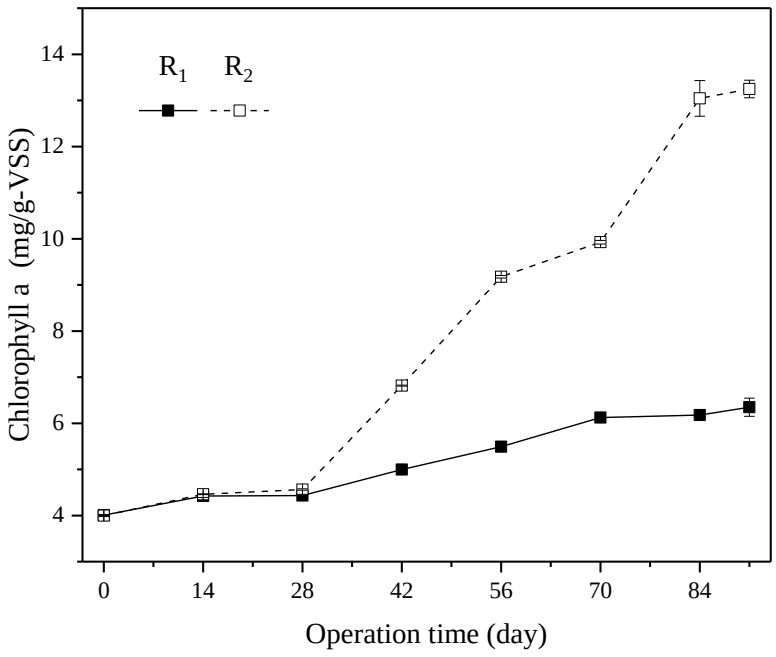

Figure 3-8 Variations of chlorophyll *a* concentration in the granules from R_1 and R_2 during the 90 days' operation. R_1-influent with constant COD/N = 8, R_2-influent with stepwise decrease of COD/N from 8 to 1.

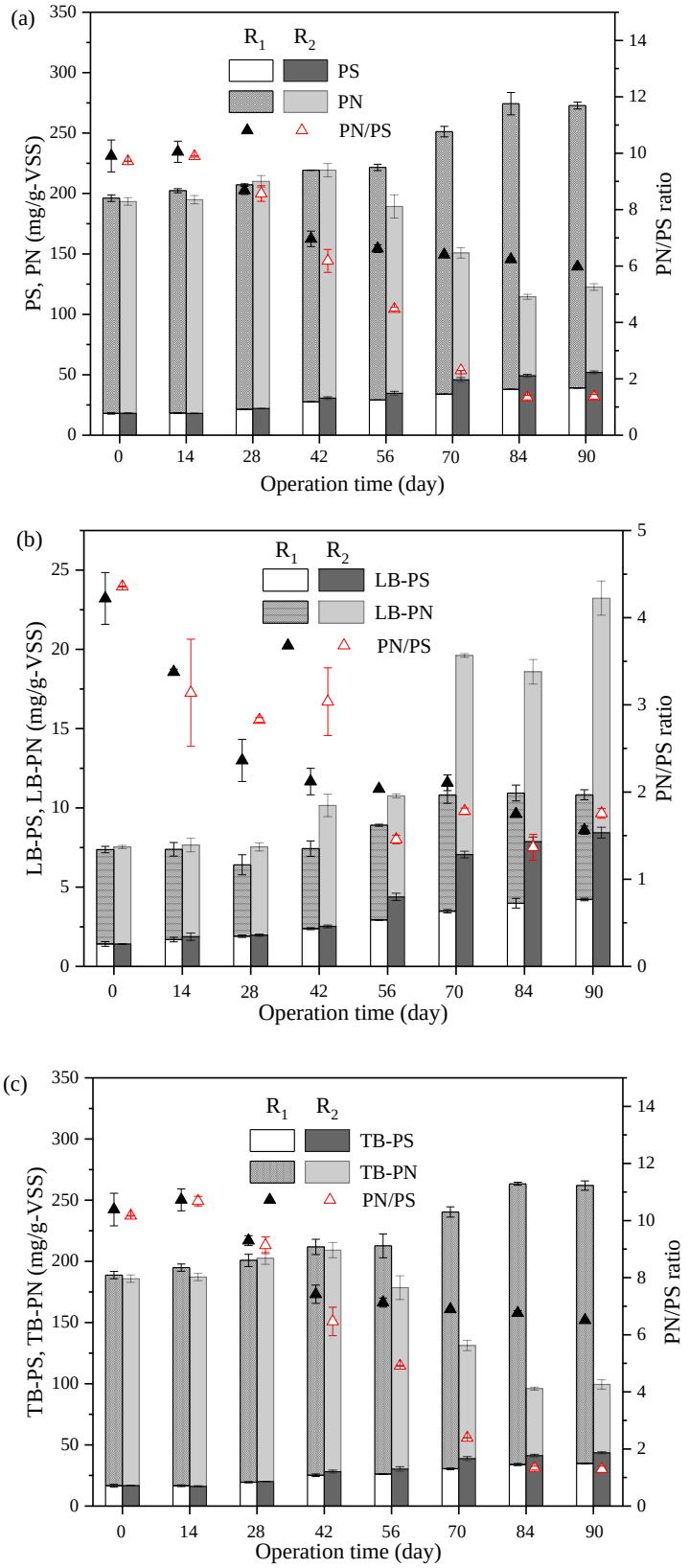

Figure 3-9 Variations of total EPS (a), LB-EPS (b), TB-EPS (c), their major components (PN and PS) and corresponding PN/PS ratios during the 90 days' operation. R_1-influent with constant COD/N = 8, R_2-influent with stepwise decrease of COD/N from 8 to 1.

still within the reported range of previous researches, possibly due to the strong and stable structure of the algal-bacterial AGS.

The changes of LB-EPS and TB-EPS contents with their major components (PN and PS) during the 90 days' operation are illustrated in Figures 3-7b and c, respectively. The trends in TB-EPS and their components in the granules from both reactors were quite similar with those of the total EPS in the granules (Figure 3-9a). The LB-EPS in the granules, however, showed a gradual increase trend for both reactors during the whole operation, in which the granules from R_2 contained much higher LB-EPS after the influent COD/N ratio was further decreased to 2 or 1. While a similar decline trend was detected in the PN/PS ratio of LB-EPS, and more specifically, not so much difference was found in the PN/PS ratio of LB-EPS in the granules from the two reactors during the operation of Stage IV. As seen from Figure 3-4c, the granules in the two reactors exhibited good stability during the whole operation, even for R_2 to which the influent COD/N ratio was decreased from 8 to 1 resulting in remarkable decrease in its granular TB-EPS content (Figure 3-9c). Therefore, LB-EPS is probably the key factor to control the deterioration of granular stability in the algal-bacterial AGS system (Zhang et al., 2016b).

3.3.5 Implication of this study

Results show that the algal-bacterial AGS system can well maintain its granular stability and stable operation when treating low carbon wastewater. More importantly, when the influent COD concentration decreased to 50 mg/L (COD/N = 1), the algal-bacterial AGS with compact and dense structure could still exhibit good granular stability. As a result, the algal-bacterial AGS system is more prospective due to its low requirement for external carbon source and reduced GHGs emission during wastewater treatment. On the other hand, the obtained biomass, or the algal-bacterial granules with high P and N contents, can be easily developed as functional materials for multiple purposes. In addition, the granules with high bioavailable P up to 98% can also be used for efficient P recovery. This work indicates that algal-bacterial AGS system is promising for the treatment of low carbon wastewaters, not only due to its low external carbon source requirement and reduced GHGs emission to some content, but also due to its great potential for production of P/N-rich granular biomass during wastewater treatment.

However, as mentioned before, future research is necessary to optimize the operation conditions for enhanced P accumulation in the granules and to quantify the reduction of GHGs emission. Besides, close attention should also be paid to the decreased N uptake and denitrification when feeding extreme low carbon wastewaters. The changes in microbial

biodiversity in the granules from the two reactors are undergoing, which is expected to shed light on the mechanisms involved and the contribution of algae and bacteria to the stable operation of the algal bacterial AGS system.

3.4 Summary

Algal-bacterial AGS kept granular stability with compact structure when coping with varying strength of organic wastewater, even at low COD/N ratio like COD/N = 1, in which LB-EPS might be the key to its structural stability. This novel system also exhibited great potential for reducing GHGs emission. The high P and N contents in algal-bacterial AGS suggest its great potential for nutrients or resources recovery from wastewater. Moreover, the high P bioavailability (98%) in the algal bacterial AGS was achieved under low influent carbon condition (COD/N = 1), further demonstrating the high potential for P recovery and reutilization from the produced algal-bacterial granular biomass.

Chapter 4 Effect of no air bubbling condition on granular stability, nutrients removal and P accumulation of the algal-bacterial AGS

4.1 Introduction

With the potential capability of nutrients uptake and O_2 generation by algae, the co-existence of algae and bacteria in wastewater treatment units is beneficial for enhanced nutrients removal efficiency at lower energy consumption. Although many efforts have been devoted to the algal-bacterial granular system, especially on energy saving via less aeration or no aeration conditions (Tiron et al., 2015; Tiron et al., 2017; Abouhend et al., 2018), previous works mainly focused on organics or nutrients removal efficiencies.

Results from Chapter 3 indicate that the algal-bacterial AGS biomass may high phosphorus (2.8-3.0%) with extremely high P bioavailability (up to 98%) under low influent carbon condition, which could be easily used for resource recovery. To the best of our knowledge, very little information is available regarding P content and its bioavailability as well as stability of algal-bacterial granules in no air bubbling systems which are usually applied for cultivation of AGS and algal-bacterial AGS.

This preliminary trail aimed to investigate the characteristics and performance of the mature algal-bacterial AGS in shaking photoreactors instead of air bubbling systems usually used for AGS or algal-bacterial AGS processes. Besides, P accumulation and its bioavailability in the algal-bacterial granules were detected. Results from this work are expected to provide basic information for the design of cost-effective systems to treat wastewater and subsequent resources recovery from the algal-bacterial AGS biomass.

4.2 Materials and methods

4.2.1 Experimental set-up and operation conditions

Six 250 mL glass flasks with a working volume of 200 mL each were shaken at 150 rpm constantly in a multi shaker (MMS-310, EYELA, Japan) at room temperature (25 ± 2°C), resulting in suspended granular biomass during shaking (Figure 4-1). Two artificial solar lights (NLSS15CBM-AC, Nikki Trading Corp., Japan) were applied to the reactors with the light intensity on the surface of the outer wall was 88-122 μmol/m^2·s when the artificial solar light was on (12 h/12 h, light-on/light-off). All the experiments were carried out without air bubbling (usually used for AGS or algal-bacterial AGS processes), in which O_2 could be provided by algae through photosynthesis during the light phase. Each cycle (12 hours)

(a)

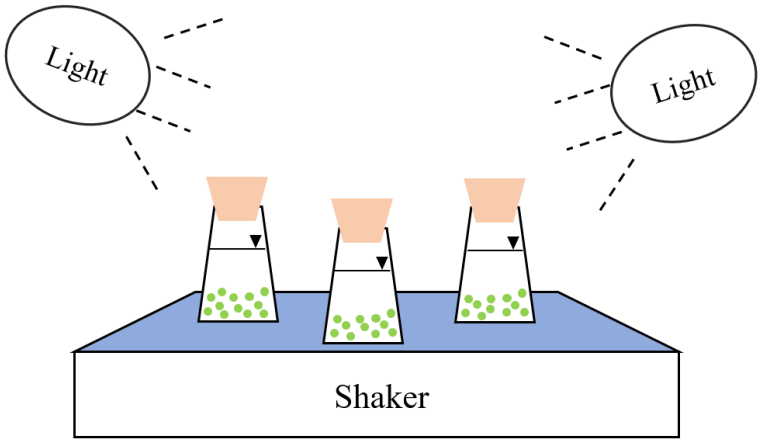

(b)

Figure 4-1 Experimental set-up (a) and the reactor (b) in this study.

consisted of 1 min filling, 715 min shaking period, 2 min settling, and 2 min effluent discharge. The volumetric exchange ratio was kept at 50%, namely, the HRT was about 24 h. SRT was kept at approximately 30 days through controlled sludge discharge. The whole test lasted for 25 days.

Synthetic wastewater used in this work was the same as the influent to R_1 in Chapter 3, mainly consisting of 400 mg COD/L, 50 mg NH_4^+-N/L, and 10 mg PO_4^{3-}-P/L. All the chemicals were supplied by Wako Pure Chemical Industries Ltd., Japan.

Prior to the present study, mature algal-bacterial AGS were cultivated in the laboratory-scale SBR which has been operated stably for more than 3 months. The dominant algae species, *Leptolyngbya*, was the same as that of algal-bacterial granules in Chapter 3. The initial concentration of MLVSS was around 3.87 ± 0.03 g/L in each photoreactor. The mean diameter of the granules was 2.32 ± 0.52 mm with a SVI_5 about 38.1 ± 0.4 mL/g.

4.2.2 Analytical methods

All the analytical methods were described elsewhere in section 2.2.2 and 3.2,2, including quantification and characterization of granular biomass (ML(V)SS, SVI, chlorophyll *a*, granular size and distribution, granular strength, P fractionation in biomass), water quality (TN, NH_4^+-N, NO_2^--N, NO_3^--N, PO_4^{3-}-P, DOC, DIC, DTC), and EPS extraction and determination.

4.2.3 Statistical analysis

All analyses were carried out in triplicate with the results being expressed as the mean ± standard deviation. Pearson's correlation analysis was performed by using Origin 2017 to clarify the correlation between P fractions and metal ions in granules. The significant difference was assumed at $p < 0.05$.

4.3 Results and discussion

4.3.1 Properties of algal-bacterial AGS in shaking photoreactors

(1) Changes in morphology and biomass retention

At the beginning, the mature algal-bacterial AGS was green, reflecting an irregular, compact and dense structure (Figure 4-2). After day 20, filamentous bacteria were observed on the outer surface of the granules. Gradually, the number of large-sized granules with superficial filamentous bacteria increased in all the reactors. Moreover, most parts of the granules turned to dark green with a larger particle diameter (3.77 ± 1.09 mm) compared to

the seed granules (2.32 ± 0.52 mm) (Table 4-1). Restated, although filamentous bacteria co-existed in the reactors till the end of experiment, no obvious disintegration was observed in the algal-bacterial granules with compact and integrated structure during the tested shaking period.

The reactors had an initial MLSS of 4.99 ± 0.06 g/L (MLVSS/MLSS = 77.6 ± 1.1%), and an obvious decrease in MLSS was detected after 25 days' operation (3.77 ± 0.12 g/L, MLVSS/MLSS = 77.6 ± 2.0%), most probably attributable to a short SRT (about 30 days) applied in this study. As it is known, chlorophyll *a* concentration can be used to represent the growth of algal biomass (Lee et al., 2015), which was detected to increase from the initial 7.99 ± 0.13 to 13.40 ± 0.01 mg/g-VSS in granules from the reactors on day 25. This observation signals the fast growth of algae in the algal-bacterial granules under the tested shaking condition.

(2) Granular settleability and stability

Effective biomass separation through the formation of fast settling biomass is one of the major advantages of AGS technology. Under the tested shaking condition, an obvious increase in SVI_5 (from 38.1 ± 0.4 to 77.5 ± 1.8 mL/g) was noticed, suggesting somewhat worsen settleability of algal-bacterial granules. This observation was partially in agreement with the finding by Abouhend et al. (2018) who attributed the increase in SVI_{30} of oxygenic photogranules to the overgrowth of filamentous green algae in stirred-tank reactors without aeration. The presence of filamentous bacteria and the low hydrodynamic shear force provided by the shaker might be the key factor for the resultant slightly lower granular settleability than the seed algal-bacteria granules, thus some decrease in granular settling velocity (from 29.1 ± 3.9 to 21.4 ± 6.2 m/h). Still, the SVI_5 of algal-bacterial AGS on day 25 was better than or comparable to the conventional AGS or algae granules in air bubbling systems (Cai et al., 2019; Wang et al., 2019).

The stability of granular sludge is a crucial factor to ensure the effluent quality from algal-bacterial granule system. In this study, granular stability was expressed in terms of integrity coefficient (%), and a lower value denotes a better stability (Muda et al., 2010). It was found that the integrity coefficient of the granules only slightly increased from the initial 7.4 ± 0.3 to 8.4 ± 0.6% on day 25, implying that the algal-bacterial AGS possesses a strong enough structure to maintain its granular stability even under constantly shaking condition.

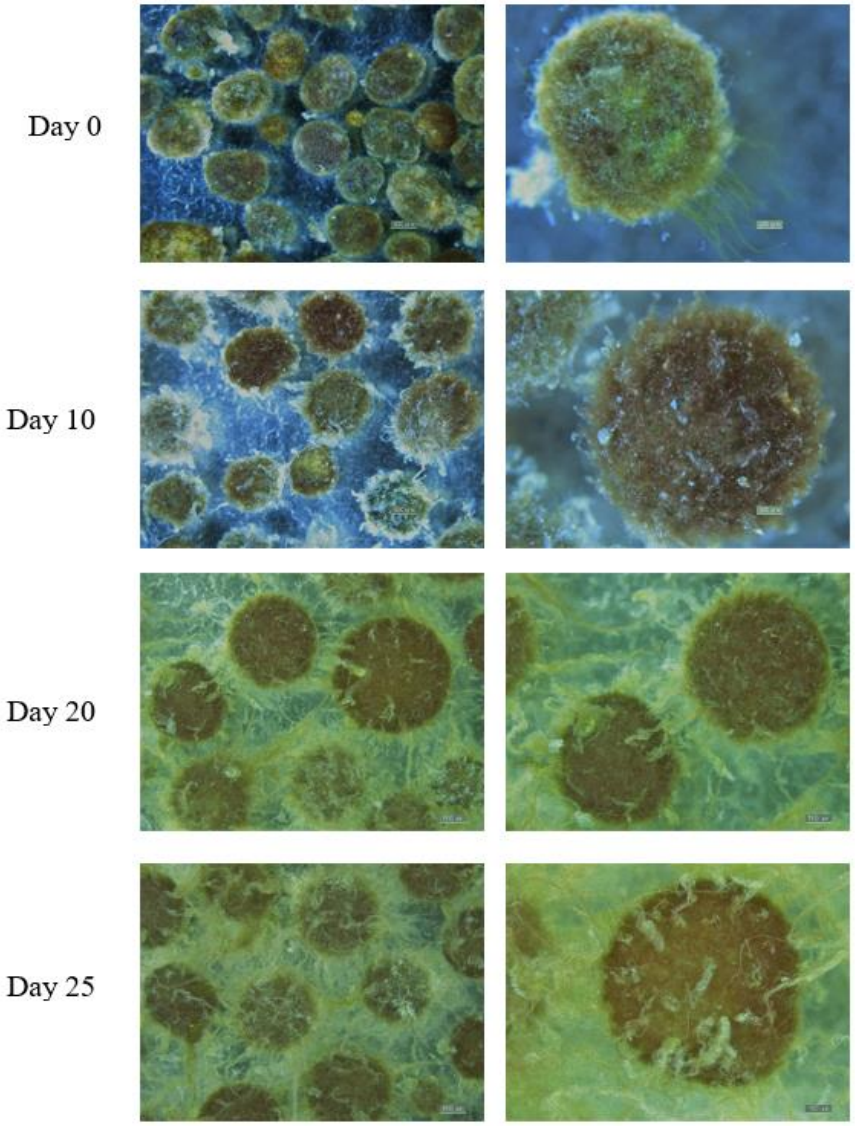

Figure 4-2 Morphological changes of the algal-bacterial AGS in shaking photoreactors on day 0, 10, 20, and 25, respectively.

Table 4-1 Comparison in characteristics of algal-bacterial AGS in the photoreactors under shaking condition between day 0 and day 25.

Parameter	Day 0	Day 25
MLSS (g/L)	4.99 ± 0.06	3.77 ± 0.12
MLVSS/MLSS (%)	77.6 ± 1.1	77.6 ± 2.0
SVI_5 (mL/g)	38.1 ± 0.4	77.5 ± 1.8
Mean diameter (mm)	2.32 ± 0.52	3.77 ± 1.09
Integrity coefficient (%)	7.4 ± 0.3	8.4 ± 0.6
Settling velocity (m/h)	29.1 ± 3.9	21.4 ± 6.2
Chlorophyll *a* (mg/g-VSS)	7.99 ± 0.13	13.40 ± 0.01

Note: ML(V)SS-mixed liquor (volatile) suspended solids, SVI_5-sludge volume index at 5 min.

4.3.2 Performance on carbon and nutrients removal

(1) DOC removal

The changes in effluent carbon concentration from the reactors were recorded during the 25 days' operation (Figure 4-3a). The effluent DOC concentration from the reactors was always < 14 mg/L from day 2 on, achieving an average DOC removal efficiency of 94.8 ± 1.6% and 94.4 ± 1.4% during the light-on and light-off cycles of the whole test period (Table 4-2). This observation indicates that the algal-bacterial AGS system could also have good performance on organics removal under shaking condition, and light illumination exhibited no obvious influence on organics removal by the algal-bacterial AGS. Similar organic removal efficiency can be achieved in the AGS systems with air bubbling AGS or algal-bacterial AGS systems (Ni et al., 2009; Ahmad et al., 2017; Cai et al., 2019). It is worth noting that enhanced DIC reduction was noticed during the light cycles from day 11 on, which might be attributable to the photosynthesis of algae. That is, light illumination can enhance DIC removal to some extent.

(2) Nitrogen and phosphorus removal

As seen from Figure 4-3b, the algal-bacterial AGS exhibited excellent performance on NH_4^+-N removal (> 99%) during light-on and light-off cycles from the very beginning of this test, indicating that stable nitrification could be quickly established in this shaking system. TN removal efficiencies in the reactors were almost at the same levels, 71.1 ± 3.3% and 69.2 ± 4.1% for light-on and light-off cycles, respectively from day 3 to the end of experiment. Compared to the study in Chapter 3 by using the same algal-bacterial AGS in the air bubbling system, a higher TN removal efficiency was detected in this study. This suggests that algal-bacterial AGS possesses great potential for N removal even under shaking condition, which could be further optimized with the relationship between DO change in bulk liquor and light illumination duration being considered. Interestingly, the TN removal efficiency in the photoreactors demonstrated an evidently increasing tendency along with the operation. This observation might be attributable to the bigger granule size with the operation, creating a more beneficial environment for denitrification (Li et al., 2017).

The effluent P concentration from the reactors during the light-on and light-off cycles, however, showed an obviously different trend (Figure 4-3c). Under 10 mg/L of influent P condition, the effluent P concentration was 4.5 ± 1.7 mg/L (varied from 2.8 to 8.5 mg/L) and 13.5 ± 4.1 mg/L (ranged between 9.1-20.9 mg/L), respectively during the light-on and light-

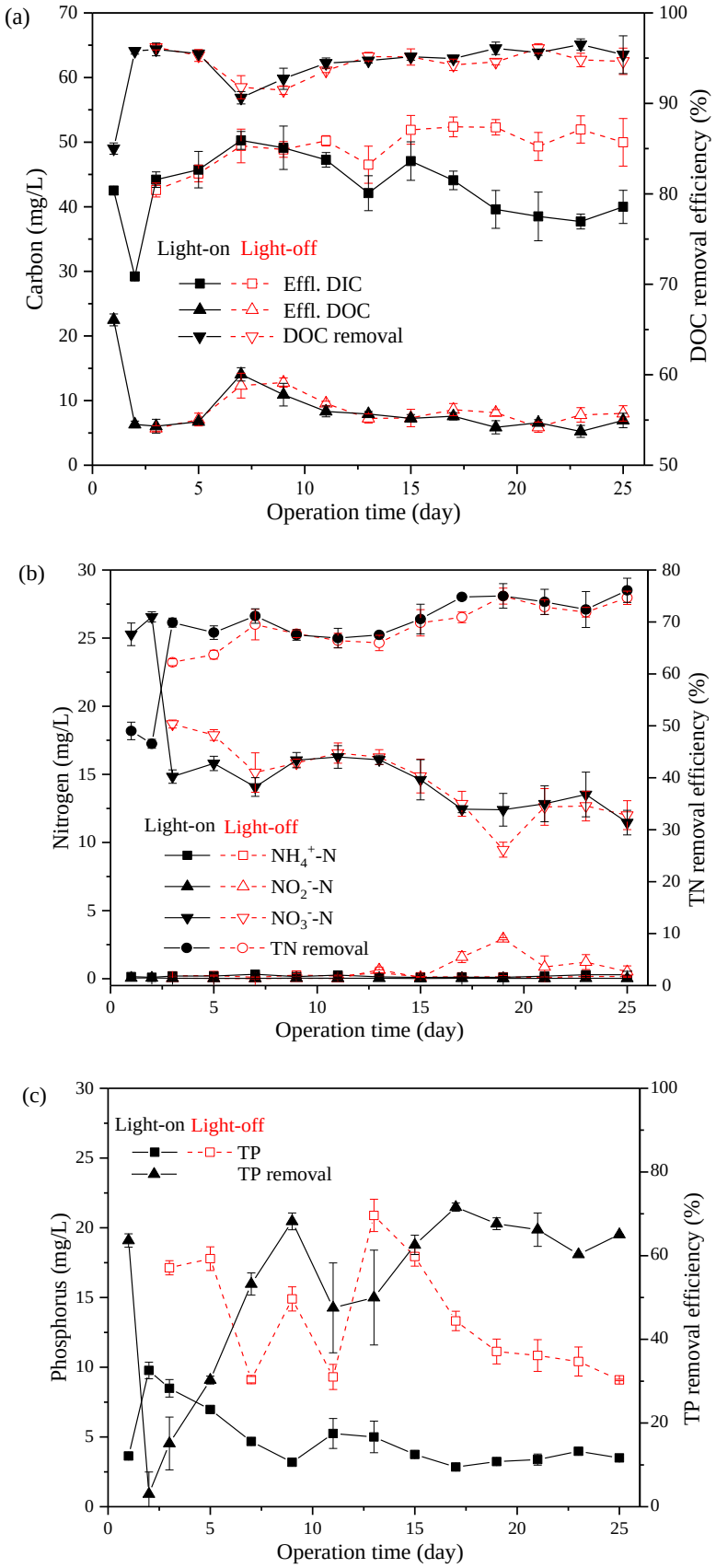

Figure 4-3 Changes in nutrients profiles during the operation: carbon (a), nitrogen (b), and phosphorus (c).

Table 4-2 Comparison in average performance between this work and the study in Chapter 3 in DOC, NH_4^+-N, TN, and TP removal efficiencies during the operation period (data after day 3).

Items	Light on			Light off			General SBR operation (R_1 in Chapter 3)		
	Max	Min	Avg	Max	Min	Avg	Max	Min	Avg
DOC removal (%)	96.5	90.6	94.8	96.2	91.5	94.4	98.9	92.7	96.2
NH_4^+-N removal (%)	99.8	99.3	99.6	99.8	99.1	99.6	100	99.7	99.9
TN removal (%)	76.1	66.9	71.1	75.0	62.2	69.2	61.2	45.6	53.8
TP removal (%)	71.6	15.1	54.8	-	-	-	81.3	40.3	66.2

Note: DOC-dissolved organic carbon, TN-total nitrogen, TP-total phosphorus.

off cycles from day 3 to the end of experiments. Botic assimilation and abiotic precipitation are reported as the main P removal means from wastewater (Nurdogan and Oswald, 1995; de Godos et al., 2009). Algae can absorb and accumulate large P quantities through luxury uptake (Solovchenko et al., 2016). In the case of algal-bacteria AGS system (Chapter 3), co-precipitation of phosphate with other co-existing metals and algae assimilation are the major contributors to P removal. As seen, almost no P removal was detected during the light-off cycles in the shaking photoreactors, suggesting algae growth and assimilation might be responsible for the enhanced P removal with light illumination in this study. Further research is necessary for the optimization on light cycle of the photoreactors to improve P uptake and effluent quality.

4.3.3 Cycle tests on day 20

In order to have a better understanding of the algal-bacterial AGS system under shaking condition, typical cycle tests (including DOC, TP, DO and N profiles) were also conducted and compared during the light-on and light-off cycles on day 20 (Figure 4-4).

After 60 min, DO concentration decreased from initial 2.7 and 2.6 mg/L to 1.37 and 0.83 mg/L during the light-on and light-off cycles, respectively. The observation indicates that the activity of aerobic bacteria (nitrifiers and heterotrophs) could be maintained in the shaking photoreactors. From 60 min on, DO increased obviously, reaching to around 8.2 and 3.5 mg/L during the light-on and light-off cycles at 720 min, respectively. For DOC concentration, light-on and light-off cycles showed a similar decrease trend, which sharply declined to 37.5 and 32.1 mg/L, respectively, at 60 min and then gradually decreased to 5.8 and 7.7 mg/L at the end of each cycle. On the other hand, the decrease of NH_4^+-N concentration in the reactors was slightly faster during the light-on cycle than that during the light-off one, indicating that besides algae assimilation, nitrification with simultaneous denitrification processes may occur under shaking and illumination conditions.

As for P, TP concentration was firstly observed to release and then uptake during the subsequent period (Figure 4-4c), suggesting that P was not only taken up by algae but also removed through PAOs in this study. Interestingly, more P release (22.6 mg/L at 120 min) during the light-off cycle was detected compared to 16.7 mg/L of P release during the light cycle (at 60 min). In addition, the effluent P concentrations were averagely about 2.5 and 10.0 mg/L at the end of light-on and light-off cycles, respectively. Almost little contribution of algal-bacterial AGS to P removal during light-off period might be attributable to the designed light-on/light-off cycle (12 h/12 h) which might not be suitable for the metabolism of PAOs. More

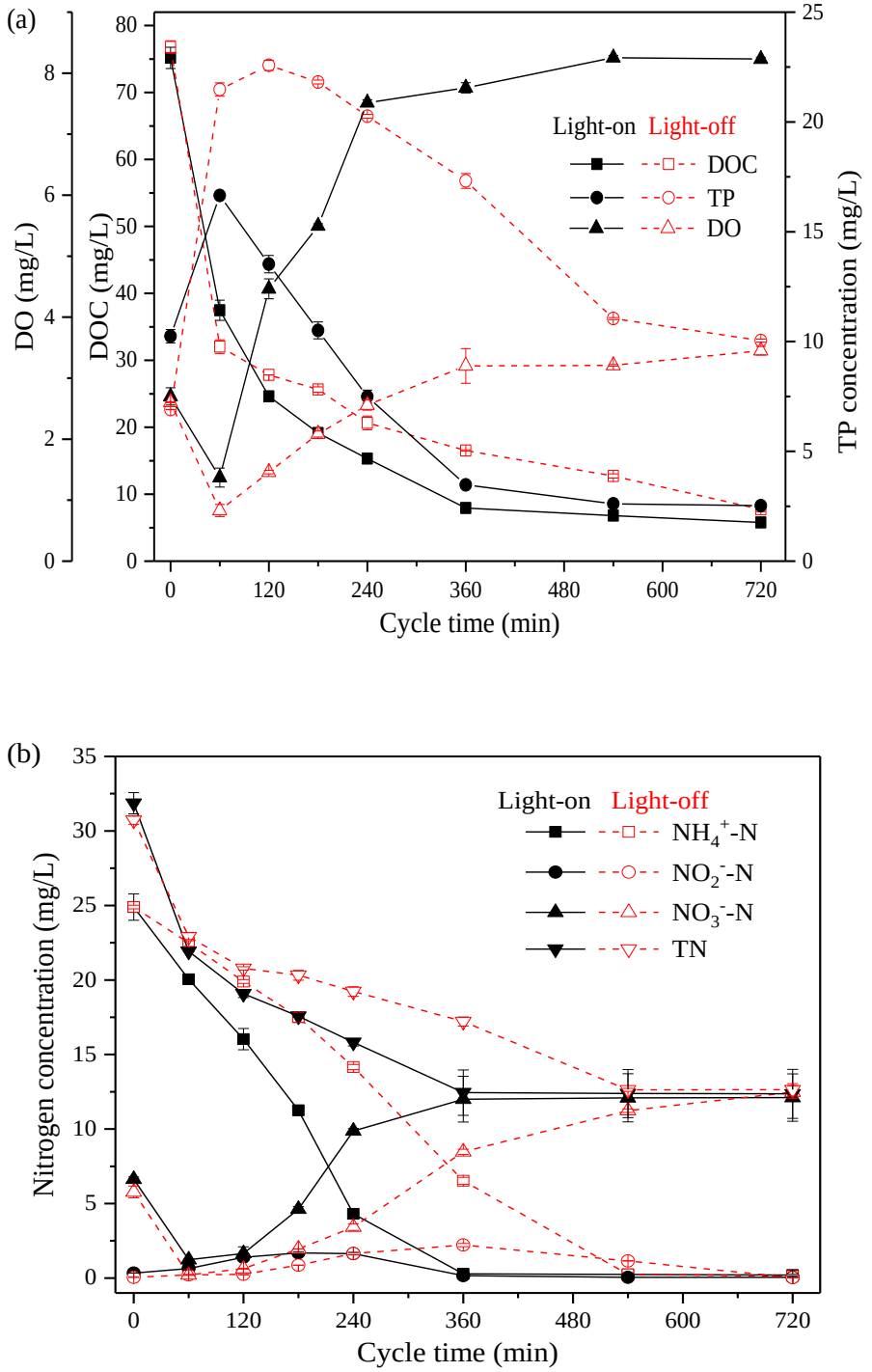

Figure 4-4 Variations of DO, DOC, and TP (a), and N species (b) in the typical light-on and light off cycles on day 20.

in-depth research is still undergoing with respect to the optimization on light-on/light-off cycle and hydraulic/sludge retention times.

4.3.4 P fractionation in algal-bacterial granules

The P fractions in granules are presented in Figure 4-5, including TP, OP, IP, NAIP and AP. It is clearly seen that the content of each P fraction in the seed algal-bacterial AGS was much higher than those in the granules on day 15 and day 25. The TP content in the granules decreased obviously, from the initial 30.4 ± 0.4 to 23.8 ± 0.3 on day 15 and to 21.5 ± 0.4 mg/g-SS on day 25, respectively. Correspondingly, the OP and NAIP contents decreased from the initial 5.8 ± 0.3 (occupying 19% of TP) and 22.5 ± 0.3 mg/g-SS (74% of TP) to 3.1 ± 0.2 and 16.7 ± 0.1 mg/g-SS on day 25, accounting for 14% and 78% of TP in the granules, respectively. However, the AP content maintained at around 1.6 ± 0.1 mg/g-SS in the granules during the whole process, signaling its relative stability in quantity under the tested condition. This observation also indicates that the decrease of TP content in the granules is mainly contributed by OP and NAIP under the shaking condition. Specifically, Fe content in the granules reflected a similar decrease trend as NAIP (Table 4-3), and a strongly positive correlation (R = 0.999) was found between the amount of Fe accumulated in the granules and its NAIP content. This result suggests that it might be difficult to maintain the stable Fe-PO_4 precipitates in the algal-bacterial granules under the tested operation condition, which needs further investigation. However, the proportion of potentially bioavailable P ((OP+NAIP)/TP) was relatively stable, which varied from the initial 93.2% to 92.0% in the granules on day 25. As a result, the tested condition has limited effect on bioavailable P in the algal-bacterial granules containing high bioavailable P.

4.3.5 EPS secretion from algal-bacterial granules

EPS play an essential role in the formation and stability of granule (Caudan et al., 2014; Guo et al., 2016). As shown in Figure 4-6. The total EPS content increased significantly from the initial 100.0 ± 1.5 mg/g-VSS to 174.5 ± 4.8 mg/g-VSS on day 25, in which PN was much more abundant than PS. During the operation PN increased from the initial 86.2 ± 1.9 to 153.7

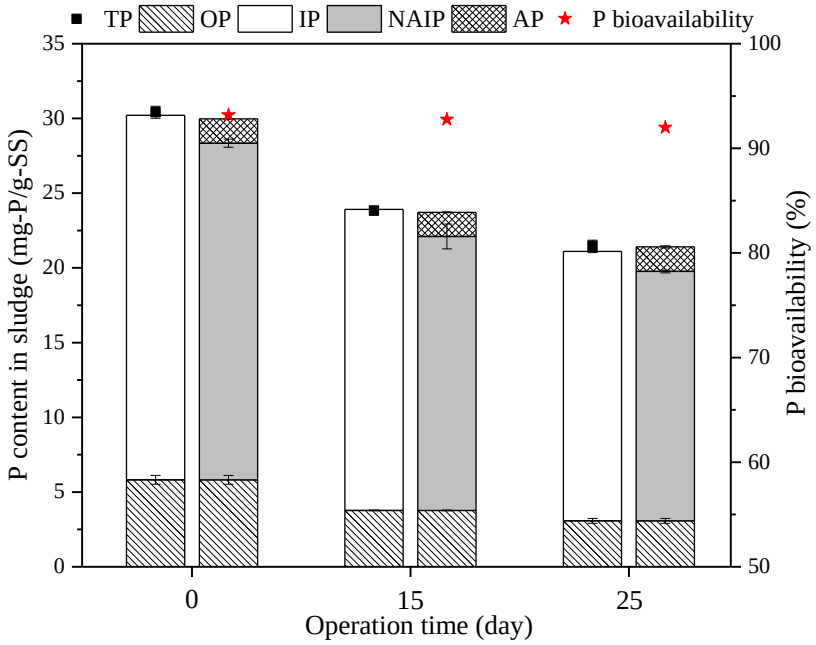

Figure 4-5 Changes in P content and its fractions in the algal-bacterial granules on day 0, day 15 and day 25. NAIP-non-apatite inorganic phosphorus, OP-organic phosphorus, AP-apatite phosphorus.

Table 4-3 Changes in average element contents in the algal-bacterial granules on day 0, day 15 and day 25 (unit: mg/g-SS).

Day	Na	K	Fe	Ca	Mg	Al
0	6.95	6.12	15.31	9.07	5.28	0.77
15	6.41	6.27	9.04	9.19	5.84	0.65
25	7.09	5.69	5.97	9.73	4.99	0.89

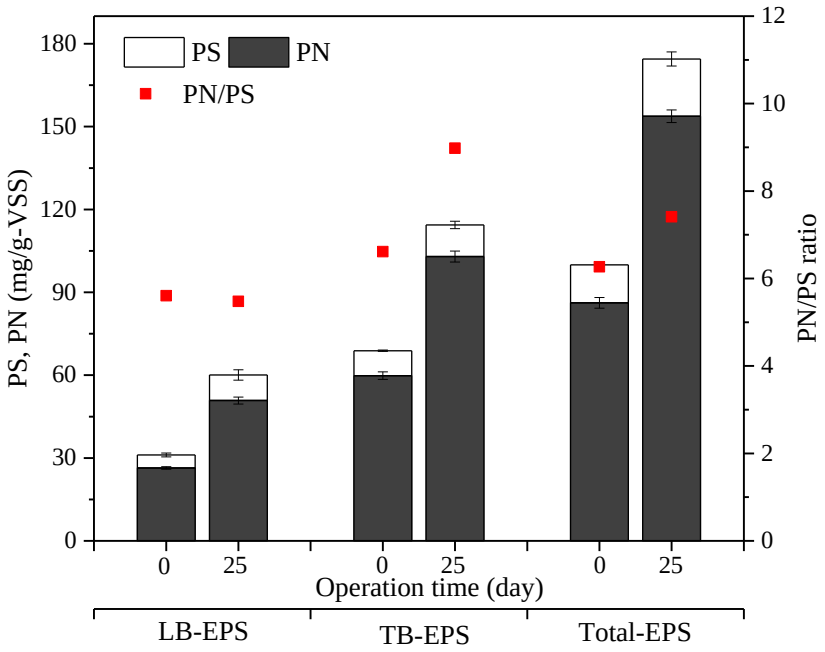

Figure 4-6 Changes in LB-EPS, TB-EPS, total EPS, their major components (PN and PS) and corresponding PN/PS ratios of algal-bacterial granules on day 0 and day 25. EPS-extracellular polymeric substances, LB-EPS-loosely bound EPS, TB-EPS-tightly bound EPS, PN-extracellular proteins, PS-extracellular polysaccharides.

± 2.3 mg/g-VSS on day 25, and the PN/PS ratio rose from 6.3 to 7.4 correspondingly. The increment in PN excretion in this study indicates that PN might function as protective agents for bacteria and maintain the stability of algal-bacterial granules under the shaking condition (Zhang et al., 2018).

Previous works indicate that EPS may have a different content distribution in the layered structure of AGS (Chen et al., 2007; Adav et al., 2008), which can be mainly divided into two different fractions, i.e. LB-EPS and TB-EPS (Li and Yang, 2007). Figure 4-6 also shows the changes of LB-EPS and TB-EPS contents with their major components (PN and PS) during the 25 days' operation. In general, the PN and PS contents in the LB-EPS and TB-EPS increased with a similar increase trend as those in the total EPS in the granules. The PN/PS ratio slightly decreased from the initial 5.6 to 5.5 in LB-EPS, whereas it increased from 6.6 to 9.0 on day 25 in TB-EPS. This observation suggests that PN in the TB-EPS is more sensitive than that in the LB-EPS in the algal-bacterial granules under the tested condition. The above results also imply that PN plays a crucial role in the maintenance of the stable inner structure of algal-bacterial AGS.

4.4 Summary

The stability and performance of mature algal-bacterial AGS was examined by using shaking photoreactors. The algal-bacterial AGS possessed good granular integrity (8.4 ± 0.6%), excellent DOC removal (94.8 ± 1.6%) and high TN removal (71.1 ± 3.3%) during 25 days' operation. The stability of Fe-PO_4 precipitates in the granules was affected to some extent under the tested conditions, during which a high P bioavailability (92.0%) was still maintained. Further research is directed to the optimization of light-on/light-off cycle and hydraulic/sludge retention times in order to realize the minimum energy consumption for wastewater treatment by using this novel algal-bacterial AGS system.

Chapter 5 Conclusions and future research perspectives

5.1 Conclusions

This study investigated the changes in granular stability and nutrients removal during wastewater treatment under low COD/N wastewater or no air bubbling condition, especially P accumulation and its bioavailability of algal-bacterial AGS. In addition, the formation of algal-bacterial AGS from mature bacterial AGS were also attempted. The main results can be summarized as follows.

(1) Stability of aerobic granules during long-term operation is still challenging its practical applications. In Chapter 2, the algal-bacterial AGS was successfully developed by seeding mature bacterial AGS under light illumination with no algae inoculation, which reflected a compact structure with higher stability (0.9-10.7%) compared with the seed bacterial AGS (10.7-15.0%). From the results of Chapter 3, the algal-bacterial AGS can maintain its granular stability (0.7-5.4%) when the influent COD/N stepwise decreased from 8 to 1, in which LB-EPS might be the key to its structural stability. As shown in Chapter 4, the algal-bacterial AGS possessed good granular integrity (8.4 ± 0.6%) under no air bubbling condition after the 25 days' operation. More extracellular PN (153.7 ± 2.3 mg/g-VSS) were excreted with a high PN/PS (~ 7.4) ratio in the algal-bacterial granules on day 25, especially the TB-PN which is mainly responsible for granular stability. These findings demonstrate the great potential of algal-bacterial AGS in the treatment of low carbon wastewater or under no air bubbling conditions, through which carbon source and energy consumption can be further reduced if algal-bacterial AGS being applied.

(2) As for nutrients removal by the algal-bacterial AGS system, higher TN (averagely 54.6%) and TP (averagely 58.4%) removal efficiencies were achieved in the algal-bacterial AGS system, in comparison to 48.3% and 54.5% respectively in the bacterial AGS system. Under lower influent COD/N ratio (2 and 1) condition (Chapter 3), even though some negative impact was noticed on the nitritation process, the algal-bacterial AGS system still exhibited stable performance on DOC, NH_4^+-N, TN and TP removals. When being applied under no air bubbling condition (Chapter 4), the algal-bacterial AGS possessed excellent DOC removal (94.8 ± 1.6%) and high TN removal (71.1 ± 3.3%) by using shaking photoreactors during the 25 days' operation. The large fluctuation in TP removal (15.1-71.6%) might be attributable to the designed light/dark cycle and hydraulic/sludge retention time. Results showed that the algal-

bacterial AGS system could efficiently remove organic matter and nutrients from the synthetic domestic wastewater under low COD/N wastewater or no air bubbling condition, which reflected its application potential in the wastewater treatment with less carbon source or energy consumption.

(3) More detailed information on P content and its bioavailability in algal-bacterial AGS is important and necessary when the produced biomass is purposefully used for agriculture as P fertilizer. Compared with the P content (36.8 mg/g-SS) and P bioavailability (85%) of the bacterial granules, higher P content (44.2 mg/g-SS) with higher P bioavailability (92%) was detected in the algal-bacterial granules (Chapter 2). In addition, the algal-bacterial AGS biomass was detected to have high P content (28.3 mg/g-SS) as well as extremely high P bioavailability (up to 98%) under the low influent carbon condition (COD/N = 1, Chapter 3). Under no air bubbling condition (Chapter 4), decrease in P content, especially NAIP relating to Fe-PO_4 precipitates in the algal-bacterial granules was detected, while a high P bioavailability (92%) was still maintained. High P content and its high bioavailability of algal-bacterial AGS imply that the produced algal-bacterial granular biomass could be used for P recovery and reuse, which can reduce the global phosphate rock demand to a great extent. This work is the first trial to investigate P accumulation and its bioavailability of algal-bacterial AGS.

The results of this study are expected to provide important and scientific data for the design and realization of algal-bacterial AGS application in practice.

5.2 Future research perspectives

With the aim to optimize the reactor performance and minimize energy requirement, further explorations regarding the algal-bacterial AGS are still necessary. The following aspects should be considered in the future research.

(1) Compared with bacterial AGS, more filamentous bacteria on the surface of granules during the algal-bacterial AGS formation period was observed. The exploration of the relationship between the filamentous bacteria and algae is important to uncover possible mechanisms involved in algal-bacterial granulation.

(2) The algal-bacterial AGS possesses high potential for P recovery from wastewater, resulting in P-rich granules with high P mobility and bioavailability. Moreover, extremely high P bioavailability in granules was achieved in this study under the low influent COD/N ratio or no air bubbling condition. In the future, the promotion mechanisms involved in the enhancement of bioavailable P accumulation should be investigated.

(3) As shown in Chapter 4, further optimization of light-on/light-off cycle and hydraulic/sludge retention times is important for better and stable P accumulation in the algal-bacterial granules with high bioavailability under no air bubbling condition.

References

Abouhend, A. S., McNair, A., Kuo-Dahab, W. C., Watt, C., Butler, C. S., Milferstedt, K., Hamelin, J., Seo, J., Gikonyo, G. J., El-Moselhy, K. M., Park, C., 2018. The oxygenic photogranule process for aeration-free wastewater treatment. Environ. Sci. Technol. 52, 3503-3511.

Adav, S. S., Lee, D. J., Show, K. Y., Tay, J. H., 2008. Aerobic granular sludge: recent advances. Biotechnol. Adv. 26, 411-423.

Adav, S. S., Lee, D.-J., 2008. Extraction of extracellular polymeric substances from aerobic granule with compact interior structure. J. Hazard. Mater. 154, 1120-1126.

Ahmad, J. S. M., Cai, W., Zhao, Z., Zhang, Z., Shimizu, K., Lei, Z., Lee, D.-J., 2017. Stability of algal-bacterial granules in continuous-flow reactors to treat varying strength domestic wastewater. Bioresour. Technol. 244, 225-233.

APHA, 2012. Standard Methods for the Examination of Water and Wastewater, American Public Health Association/American Water Work Association/Water Environment Federation, Washington, D.C., USA.

Beun, J. J., van Loosdrecht, M. C. M., Heijnen, J. J., 2002. Aerobic granulation in a sequencing batch airlift reactor. Water Res. 36, 702-712.

Boelee, N. C., Temmink, H., Janssen, M., Buisman, C. J. N., Wijffels, R. H., 2014. Balancing the organic load and light supply in symbiotic microalgal-bacterial biofilm reactors treating synthetic municipal wastewater. Ecol. Eng. 64, 213-221.

Cai, W., Huang, W., Li, H., Sun, B., Xiao, H., Zhang, Z., Lei, Z., 2016. Acetate favors more phosphorus accumulation into aerobic granular sludge than propionate during the treatment of synthetic fermentation liquor. Bioresour. Technol. 214, 596-603.

Cai, W., Zhao, Z., Li, D., Lei, Z., Zhang, Z., Lee, D. J., 2019. Algae granulation for nutrients uptake and algae harvesting during wastewater treatment. Chemosphere 214, 55-59.

Caudan, C., Filali, A., Spérandio, M., Girbal-Neuhauser, E., 2014. Multiple EPS interactions involved in the cohesion and structure of aerobic granules. Chemosphere 117, 262-270.

Chen, M. Y., Lee, D. J., Tay, J. H., 2007. Distribution of extracellular polymeric substances in aerobic granules. Appl. Microbiol. Biotechnol. 73, 1463-1469.

Cordell, D., Drangert, J. O., White, S., 2009. The story of phosphorus: global food security and food for thought. Global Environ. Chang. 19, 292-305.

de Godos, I., Blanco, S., García-Encina, P. A., Becares, E., Muñoz, R., 2009. Long-term operation of high rate algal ponds for the bioremediation of piggery wastewaters at high

loading rates. Bioresour. Technol. 100, 4332-4339.

Fernández, F. J., Castro, M. C., Rodrigo, M. A., Canizares, P., 2011. Reduction of aeration costs by tuning a multi-set point on/off controller: A case study. Control Eng. Pract. 19, 1231-1237.

Ghangrekar, M. M., Asolekar, S. R., Joshi, S. G., 2005. Characteristics of sludge developed under different loading conditions during UASB reactor start-up and granulation. Water Res. 39, 1123-1133.

Gong, B., Wang, Y., Wang, J., Huang, W., Zhou, J., He, Q., 2018. Intensified nitrogen and phosphorus removal by embedding electrolysis in an anaerobic-anoxic-oxic reactor treating low carbon/nitrogen wastewater. Bioresour. Technol. 256, 562-565.

Guo, J., Wang, S., Lian, J., Ngo, H. H., Guo, W., Liu, Y., Song, Y., 2016. Rapid start-up of the anammox process: Effects of five different sludge extracellular polymeric substances on the activity of anammox bacteria. Bioresour. Technol. 220, 641-646.

He, Q., Chen, L., Zhang, S., Chen, R., Wang, H., Zhang, W., Song, J., 2018. Natural sunlight induced rapid formation of water-born algal-bacterial granules in an aerobic bacterial granular photo-sequencing batch reactor. J. Hazard. Mater. 359, 222-230.

Herbert, D., Phipps, P. J., Strange, R. E., 1971. Chapter III: Chemical analysis of microbial cells. In: Methods in Microbiology, (Eds.) J. R. Norris, D. W. Ribbons, Volume 5, Part B, Academic Press, pp. 209-344.

Hu, Y., Hao, X., van Loosdrecht, M., Chen, H., 2017. Enrichment of highly settleable microalgal consortia in mixed cultures for effluent polishing and low-cost biomass production. Water Res. 125, 11-22.

Huang, W., Li, B., Zhang, C., Zhang, Z., Lei, Z., Lu, B., Zhou, B., 2015a. Effect of algae growth on aerobic granulation and nutrients removal from synthetic wastewater by using sequencing batch reactors. Bioresour. Technol. 179, 187-192.

Huang, W., Cai, W., Huang, H., Lei, Z., Zhang, Z., Tay, J. H., Lee, D.-J., 2015b. Identification of inorganic and organic species of phosphorus and its bio-availability in nitrifying aerobic granular sludge. Water Res. 68, 423-431.

Kocaturk, I., Erguder, T. H., 2016. Influent COD/TAN ratio affects the carbon and nitrogen removal efficiency and stability of aerobic granules. Ecol. Eng. 90, 12-24.

Lee, C. S., Lee, S. A., Ko, S. R., Oh, H. M., Ahn, C. Y., 2015. Effects of photoperiod on nutrient removal, biomass production, and algal-bacterial population dynamics in lab-scale photobioreactors treating municipal wastewater. Water Res. 68, 680-691.

Lee, D.-J., Chen, Y. Y., Show, K. Y., Whiteley, C. G., Tay, J. H., 2010. Advances in aerobic granule formation and granule stability in the course of storage and reactor operation. Biotechnol. Adv. 28, 919-934.

Li, B., Huang, W., Zhang, C., Feng, S., Zhang, Z., Lei, Z., Sugiura, N., 2015. Effect of TiO_2 nanoparticles on aerobic granulation of algal-bacterial symbiosis system and nutrients removal from synthetic wastewater. Bioresour. Technol. 187, 214-220.

Li, J., Ding, L. B., Cai, A., Huang, G. X., Horn, H., 2014. Aerobic sludge granulation in a full-scale sequencing batch reactor. BioMed Res. Int. 2014, 268789.

Li, X. Y., Yang, S. F., 2007. Influence of loosely bound extracellular polymeric substances (EPS) on the flocculation, sedimentation and dewaterability of activated sludge. Water Res. 41, 1022-1030.

Li, X., Luo, J., Guo, G., Mackey, H. R., Hao, T., Chen, G., 2017. Seawater-based wastewater accelerates development of aerobic granular sludge: a laboratory proof-of-concept. Water Res. 115, 210-219.

Liao, R., Shen, K., Li, A. M., Shi, P., Li, Y., Shi, Q., Wang, Z., 2013. High-nitrate wastewater treatment in an expanded granular sludge bed reactor and microbial diversity using 454 pyrosequencing analysis. Bioresour. Technol. 134, 190-197.

Lim, Y. W., Lee, S. A., Kim, S. B., Yong, H. Y., Yeon, S. H., Park, Y. K., Jeong D. W., Park, J. S., 2005. Diversity of denitrifying bacteria isolated from Daejeon sewage treatment plant. J. Microbiol. 43, 383-390.

Lin, Y. M., Bassin, J. P., van Loosdrecht, M. C. M., 2012. The contribution of exopolysaccharides induced struvites accumulation to ammonium adsorption in aerobic granular sludge. Water Res. 46, 986-992.

Liu, Y. Q., Tay, J. H., 2015. Fast formation of aerobic granules by combining strong hydraulic selection pressure with overstressed organic loading rate. Water Res. 80, 256-266.

Liu, L., Fan, H., Liu, Y., Liu, C., Huang, X., 2017. Development of algae-bacteria granular consortia in photo-sequencing batch reactor. Bioresour. Technol. 232, 64-71.

Liu, L., Zeng, Z., Bee, M., Gibson, V., Wei, L., Huang, X., Liu, C., 2018a. Characteristics and performance of aerobic algae-bacteria granular consortia in a photo-sequencing batch reactor. J. Hazard. Mater. 349, 135-142.

Liu, L., Hong, Y., Ye, X., Wei, L., Liao, J., Huang, X., Liu, C., 2018b. Biodiesel production from microbial granules in sequencing batch reactor. Bioresour. Technol. 249, 908-915.

Liu, Q. S., Tay, J. H., Liu, Y., 2003. Substrate concentration-independent aerobic granulation in

sequential aerobic sludge blanket reactor. Environ. Technol. 24, 1235-1242.

Lowry, O. H., Rosebrough, N. J., Farr, A. L., Randall, R. J., 1951. Protein measurement with the Folin phenol reagent. J. Biol. Chem. 193, 265-275.

Luo, J., Hao, T., Wei, L., Mackey, H. R., Lin, Z., Chen, G. H., 2014. Impact of influent COD/N ratio on disintegration of aerobic granular sludge. Water Res. 62, 127-135.

Meng, F., Xi, L., Liu, D., Huang, W., Lei, Z., Zhang, Z., Huang, W., 2019. Effects of light intensity on oxygen distribution, lipid production and biological community of algal-bacterial granules in photo-sequencing batch reactors. Bioresour. Technol. 272, 473-481.

Miao, L., Wang, S., Cao, T., Peng, Y., Zhang, M., Liu, Z., 2016. Advanced nitrogen removal from landfill leachate via anammox system based on sequencing biofilm batch reactor (SBBR): Effective protection of biofilm. Bioresour. Technol. 220, 8-16.

Mishima, K., Nakamura, M., 1991. Self-immobilization of aerobic activated sludge - a pilot study of the aerobic upflow sludge blanket process in municipal sewage treatment. Water Sci. Technol. 23, 981-990.

Morgenroth, E., Sherden, T., van Loosdrecht, M. C. M., Heijnen, J. J., Wilderer, P. A., 1997. Aerobic granular sludge in a sequencing batch reactor. Water Res. 31, 3191-3194.

Muda, K., Aris, A., Salim, M. R., Ibrahim, Z., Yahya, A., van Loosdrecht, M. C., Nawahwi, M. Z., 2010. Development of granular sludge for textile wastewater treatment. Water Res. 44, 4341-4350.

Mulbry, W., Westhead, E. K., Pizarro, C., Sikora, L., 2005. Recycling of manure nutrients: use of algal biomass from dairy manure treatment as a slow release fertilizer. Bioresour. Technol. 96, 451-458.

Mulbry, W., Kondrad, S., Pizarro, C., 2007. Biofertilizers from algal treatment of dairy and swine manure effluents: characterization of algal biomass as a slow release fertilizer. J. Vegetable Sci. 12, 107-125.

Ni, B. J., Xie, W. M., Liu, S. G., Yu, H. Q., Wang, Y. Z., Wang, G., Dai, X. L., 2009. Granulation of activated sludge in a pilot-scale sequencing batch reactor for the treatment of low-strength municipal wastewater. Water Res. 43, 751-761.

Nurdogan, Y., Oswald, W. J., 1995. Enhanced nutrient removal in high-rate ponds. Water Sci. Technol. 31, 33-43.

Oehmen, A., Lemos, P. C., Carvalho, G., Yuan, Z., Keller, J., Blackall, L. L., Reis, M. A., 2007. Advances in enhanced biological phosphorus removal: from micro to macro scale. Water Res. 41, 2271-2300.

Pardo, P., Lopez-Sanchez, J. F., Rauret, G., 2003. Relationships between phosphorus fractionation and major components in sediments using the SMT harmonised extraction procedure. Anal. Bioanal. Chem. 376, 248-254.

Pronk, M., De Kreuk, M. K., De Bruin, B., Kamminga, P., Kleerebezem, R. V., van Loosdrecht, M. C. M., 2015. Full scale performance of the aerobic granular sludge process for sewage treatment. Water Res. 84, 207-217.

Quijano, G., Arcila, J. S., Buitrón, G., 2017. Microalgal-bacterial aggregates: applications and perspectives for wastewater treatment. Biotechnol. Adv. 35, 772-781.

Rosso, D., Larson, L. E., Stenstrom, M. K., 2008. Aeration of large-scale municipal wastewater treatment plants: state of the art. Water Sci. Technol. 57, 973-978.

Ruban, V., López-Sánchez, J. F., Pardo, P., Rauret, G., Muntau, H., Quevauviller, P., 1999. Selection and evaluation of sequential extraction procedures for the determination of phosphorus forms in lake sediment. J. Environ. Monit. 1, 51-56.

Santiago, A. F., Calijuri, M. L., Assemany, P. P., Calijuri, M. D. C., Reis, A. J. D. D., 2013. Algal biomass production and wastewater treatment in high rate algal ponds receiving disinfected effluent. Environ. Technol. 34, 1877-1885.

Sforza, E., Pastore, M., Sanchez, S.S., Bertucco, A., 2018. Bioaugmentation as a strategy to enhance nutrient removal: Symbiosis between *Chlorella protothecoides* and *Brevundimonas diminuta*. Bioresour. Technol. Rep. 4, 153-158.

Shimura, Y., Hirose, Y., Misawa, N., Osana, Y., Katoh, H., Yamaguchi, H., Kawachi, M., 2015. Comparison of the terrestrial cyanobacterium *Leptolyngbya* sp. NIES-2104 and the freshwater *Leptolyngbya boryana* PCC 6306 genomes. DNA Res. 22, 403-412.

Solovchenko, A., Verschoor, A. M., Jablonowski, N. D., Nedbal, L., 2016. Phosphorus from wastewater to crops: an alternative path involving microalgae. Biotechnol. Adv. 34, 550-564.

Świątczak, P., Cydzik-Kwiatkowska, A., 2018. Performance and microbial characteristics of biomass in a full-scale aerobic granular sludge wastewater treatment plant. Environ. Sci. Pollut. Res. 25, 1655-1669.

Tang, C. C., Zuo, W., Tian, Y., Sun, N., Wang, Z. W., Zhang, J., 2016. Effect of aeration rate on performance and stability of algal-bacterial symbiosis system to treat domestic wastewater in sequencing batch reactors. Bioresour. Technol. 222, 156-164.

Tiron, O., Bumbac, C., Patroescu, I. V., Badescu, V. R., Postolache, C., 2015. Granular activated algae for wastewater treatment. Water Sci. Technol. 71, 832-839.

Tiron, O., Bumbac, C., Manea, E., Stefanescu, M., Lazar, M. N., 2017. Overcoming microalgae harvesting barrier by activated algae granules. Sci. Rep. 7, 4646.

van Loosdrecht, M. C., Brdjanovic, D., 2014. Anticipating the next century of wastewater treatment. Science 344, 1452-1453.

Wang, D., Fu, Q., Xu, Q., Liu, Y., Ngo, H.H., Yang, Q., Zeng, G., Li, X., Ni, B.-J., 2017. Free nitrous acid-based nitrifying sludge treatment in a two-sludge system enhances nutrient removal from low-carbon wastewater. Bioresour. Technol. 244, 920-928.

Wang, X., Chen, Z., Shen, J., Zhao, X., Kang, J., 2019. Impact of carbon to nitrogen ratio on the performance of aerobic granular reactor and microbial population dynamics during aerobic sludge granulation. Bioresour. Technol. 271, 258-265.

Xie, C., Zhao, J., Tang, J., Xu, J., Lin, X., Xu, X., 2011. The phosphorus fractions and alkaline phosphatase activities in sludge. Bioresour. Technol. 102, 2455-2461.

Ye, Y., Ngo, H. H., Guo, W., Liu, Y., Zhang, X., Guo, J., Ni, B., Chang, S. W., Nguyen, D. D., 2016. Insight into biological phosphate recovery from sewage. Bioresour. Technol. 218, 874-881.

Zhang, B., Ji, M., Qiu, Z., Liu, H., Wang, J., Li, J., 2011. Microbial population dynamics during sludge granulation in an anaerobic-aerobic biological phosphorus removal system. Bioresour. Technol. 102, 2474-2480.

Zhang, B., Lens, P. N., Shi, W., Zhang, R., Zhang, Z., Guo, Y., Cui, F., 2018. Enhancement of aerobic granulation and nutrient removal by an algal-bacterial consortium in a lab-scale photobioreactor. Chem. Eng. J. 334, 2373-2382.

Zhang, Q., Hu, J., Lee, D. J., 2016a. Aerobic granular processes: current research trends. Bioresour. Technol. 210, 74-80.

Zhang, Y., Ma, H., Niu, Q., Chen, R., Hojo, T., Li, Y. Y., 2016b. Effects of substrate shock on extracellular polymeric substance (EPS) excretion and characteristics of attached biofilm anammox granules. RSC Adv. 6, 113289-113297.

Zhong, Z., Wu, X., Gao, L., Lu, X., Zhang, B., 2016. Efficient and microbial communities for pollutant removal in a distributed-inflow biological reactor (DBR) for treating piggery wastewater. RSC Adv. 6, 95987-95998.

Zhou, D., Zhang, C., Fu, L., Xu, L., Cui, X., Li, Q., Crittenden, J. C., 2017. Responses of the microalga *Chlorophyta* sp. to bacterial quorum sensing molecules (N-acylhomoserine lactones): Aromatic protein-induced self-aggregation. Environ. Sci. Technol. 51, 3490-3498.

Acknowledgements

I would like to deliver my greatest gratitude to my supervisors, Professors Zhenya Zhang and Zhongfang Lei, for providing me the opportunity to undertake this research, and for their enthusiasm, encouragement, determination and depth of knowledge.

Special thanks should go to my thesis committee members, Professors Zhenya Zhang, Zhongfang Lei, Kazuya Shimizu and Motoo Utsumi for their patient reading and listening, valuable suggestions and comments. Furthermore, I shall extent my gratefulness to Professor Takeshi Mizunoya for his valuable comments for my research during the past three years.

I also cannot forget my colleagues and friends. Especially, I wish to express my appreciation to Dr. Wei Cai, Dr. Ahmad Johan Syafri Mahathir, Dr. Yang Yu, Mr. Sen Liu and other friends for their countless assistance and encouragement during the three years of my research.

The deepest gratitude goes to my family for their priceless love and support. Special thanks to my wife (Yang Xiaojing), little princess (Nian Nian) and parents for their endless love and care. This dissertation would not have been completed without their love, care, and unselfish support.

Publications

1. **Zhao, Z.**, Yang, X., Cai, W., Lei, Z., Shimizu, K., Zhang, Z., Utsumi, M., Lee, D. J., 2018. Response of algal-bacterial granular system to low carbon wastewater: Focus on granular stability, nutrients removal and accumulation. Bioresour. Technol. 268, 221-229.
2. Huang, W., **Zhao, Z. (co-first author)**, Yuan, T., Yu, Y., Huang, W., Lei, Z., Zhang, Z., 2018. Enhanced dry anaerobic digestion of swine excreta after organic nitrogen being recovered as soluble proteins and amino acids using hydrothermal technology. Biomass Bioenergy 108, 120-125.
3. Cai, W., **Zhao, Z.**, Li, D., Lei, Z., Zhang, Z., Lee, D. J., 2019. Algae granulation for nutrients uptake and algae harvesting during wastewater treatment. Chemosphere 214, 55-59.
4. Huang, W., **Zhao, Z.**, Yuan, T., Huang, W., Lei, Z., Zhang, Z., 2017. Low-temperature hydrothermal pretreatment followed by dry anaerobic digestion: A sustainable strategy for manure waste management regarding energy recovery and nutrients availability. Waste Manage. 70, 255-262.
5. Huang, W., **Zhao, Z.**, Yuan, T., Lei, Z., Cai, W., Li, H., Zhang, Z., 2016. Effective ammonia recovery from swine excreta through dry anaerobic digestion followed by ammonia stripping at high total solids content. Biomass Bioenergy 90, 139-147.
6. Chen, K., **Zhao, Z.**, Yang, X., Lei, Z., Zhang, Z., Zhang, S., 2018. Desorption trials and granular stability of chromium loaded aerobic granular sludge from synthetic domestic wastewater treatment. Bioresour. Technol. Rep. 1, 9-15.
7. Ahmad, J. S. M., Cai, W., **Zhao, Z.**, Zhang, Z., Shimizu, K., Lei, Z., Lee, D.-J., 2017. Stability of algal-bacterial granules in continuous-flow reactors to treat varying strength domestic wastewater. Bioresour. Technol. 244, 225-233.
8. Huang, W., Yuan, T., **Zhao, Z.**, Yang, X., Huang, W., Zhang, Z., Lei, Z., 2016. Coupling hydrothermal treatment with stripping technology for fast ammonia release and effective nitrogen recovery from chicken manure. ACS Sustainable Chem. Eng. 4, 3704-3711.
9. Cai, W., Jin, M., **Zhao, Z.**, Lei, Z., Zhang, Z., Adachi, Y., Lee, D. J., 2018. Influence of ferrous iron dosing strategy on aerobic granulation of activated sludge and bioavailability of phosphorus accumulated in granules. Bioresour. Technol. Rep. 2, 7-14.

10. Huang, W., Huang, W., Yuan, T., **Zhao, Z.**, Cai, W., Zhang, Z., Lei, Z., Feng, C., 2016. Volatile fatty acids (VFAs) production from swine manure through short-term dry anaerobic digestion and its separation from nitrogen and phosphorus resources in the digestate. Water Res. 90, 344-353.
11. Yuan, T., Huang, W., Lei, Z., **Zhao, Z.**, Zhang, Z., 2017. Effects of different alkalis on hydrolysis of swine manure during dry anaerobic digestion and resultant nutrients availability. Int. Biodeterior. Biodegrad. 123, 138-145.